

The Effects of Metallicity on the Cepheid P-L Relation and the Consequences for the Extragalactic Distance Scale

Paul D. Allen^{1,2} and Tom Shanks¹

¹ *Department of Physics, Science Laboratories, South Road, Durham DH1 3LE.*

² *Astrophysics, University of Oxford, Keble Road, Oxford OX1 3RH.*

16 November 2018

ABSTRACT

If a Cepheid luminosity at given period depends on metallicity, then the P-L relation in galaxies with higher metallicities may show a higher dispersion if these galaxies also sample a wider range of intrinsic metallicities. Using published HST Cepheid data from 25 galaxies, we have found such a correlation between the P-L dispersion and host galaxy metallicity which is significant at the $\approx 3\sigma$ level in the V band. In the I band the correlation is less significant, although the tighter intrinsic dispersion of the P-L relation in I makes it harder to detect such a correlation in the HST sample. We find that these results are unlikely to be explained by increased dust absorption in high metallicity galaxies. The data support the suggestion of Hoyle et al. that the metallicity dependence of the Cepheid P-L relation may be stronger than expected, with $\Delta M/[O/H] \approx -0.66$ mag dex⁻¹ at fixed period.

The high observed dispersions in the HST Cepheid P-L relations have the further consequence that the bias due to incompleteness in the P-L relation at faint magnitudes is more significant than previously thought. Using a maximum likelihood technique which takes into account the effect on the P-L relations of truncation by consistently defined magnitude completeness limits, we re-derive the Cepheid distances to the 25 galaxies and find that the average distance is increased by ≈ 0.1 mag. However, in the cases of two high metallicity galaxies at large distances the effect is severe, with the published distance modulus underestimating the true distance modulus by ≈ 0.5 mag.

In the HST sample, galaxies at higher distance tend to have higher metallicity. This means that when a full metallicity correction is made, a scale error in the published Cepheid distances is seen in the sense that the published distance moduli are increasingly underestimate at larger distances, with the average difference now being ≈ 0.3 mag. This results in the average distance modulus to the four galaxies in the Virgo cluster core increasing from $(m - M)_0 = 31.2 \pm 0.19$ to $(m - M)_0 = 31.8 \pm 0.17$ with similar increases for the Fornax and Ursa Major clusters. For the 18 HST galaxies with good Tully-Fisher distances and $m - M_0 > 29.5$ the Cepheid-TF distance modulus average residual increases from 0.44 ± 0.09 mag to 0.82 ± 0.1 mag indicating a significant scale error in TF distances and resulting in the previous Pierce & Tully TF estimate of $H_0 = 85 \pm 10$ kms⁻¹Mpc⁻¹ reducing to $H_0 = 58 \pm 7$ kms⁻¹Mpc⁻¹, assuming a still uncertain Virgo infall model. Finally, for the 8 HST galaxies with SNIa, the metallicity corrected Cepheid distances now imply a metallicity dependence of SNIa peak luminosity in the sense that metal-poor hosts have lower luminosity SNIa. Thus SNIa Hubble diagram estimates of both H_0 and q_0 may also require significant metallicity corrections.

Key words: Cepheids; Metallicity, Distance Scale, Hubble’s Constant

1 INTRODUCTION

Over fifty years after the discovery of the expansion of the universe, the value of the expansion rate, H_0 is yet to be determined to high accuracy. Although there is a general

consensus amongst astronomers that it lies somewhere between 40 and 100 kms⁻¹ Mpc⁻¹ and probably between 50 and 70 kms⁻¹ Mpc⁻¹, no conclusive result has yet been obtained. The Hubble constant is a fundamental cosmological

parameter, and its value is important for the determination of the age, density and ultimate fate of the universe. H_0 is usually measured by calculating the gradient of redshift against distance for a sample of galaxies. However, the Hubble redshift of galaxies can only be accurately determined at higher redshifts where the contribution of peculiar motions are proportionately smaller and here the measurement of extragalactic distances becomes increasingly difficult.

The primary extragalactic distance indicators are the Cepheid variables. Although there are several standard candle techniques used to measure extragalactic distances, most are calibrated using the Cepheid distances to nearby galaxies. Accurate Cepheid distances, which are free from systematic errors are therefore vitally important to determinations of H_0 .

The Hubble Space Telescope has allowed new measurements of Cepheid distances to many galaxies outside the Local Group and several groups have attempted to measure H_0 using these distances. The aim of the largest group, (the HST Key Project on the Extragalactic Distance Scale) is to calculate H_0 with an accuracy of 10%. If this is to be achieved, then several possible sources of systematic error need to be looked at in detail. These include the Cepheid P-L calibration in the LMC. A recent recalibration (Feast and Catchpole 1997) could cause H_0 to decrease by $\approx 10\%$ (Webb 1999).

In this paper we first check the effects of metallicity on the dispersion of the Cepheid P-L relation, using data from the H_0 Key Project. Then we systematically apply cuts to the data in period, in order to investigate the effects on the dispersion/metallicity relationship. We also discuss the possible causes of what is observed. We then investigate the consequences of both a global metallicity correction and the effects of bias due to incompleteness at faint magnitudes. We use a maximum likelihood technique to fit P-L relations truncated due to magnitude incompleteness and hence derive new Cepheid distances.

2 DATA

The data analysed in this work is from sources that have been either published or accepted for publication. In total, results for 25 galaxies were examined. Of these, 18 were from the ‘HST Key Project on the extragalactic distance scale’ team. The photometry and Cepheid periods are used as published. Most of this data was taken from the Key Project archive website (<http://www.ipac.caltech.edu/H0kp>). This gives the photometry/period data for the Cepheids in each of the galaxies. This was used along with published papers to obtain exactly the same data as was used by the key project team in their distance determinations. The references are as follows: NGC 925 (Silbermann et al 1996); NGC 1326A (Prosser et al 2000); NGC 1365 (Silbermann et al 1999); NGC 1425 (Mould et al 2000); NGC2090 (Phelps et al 1998); NGC 2541 (Ferrarese et al 1998); NGC 3031 (Freedman 1994); NGC 3198 (Kelson et al 1999); NGC 3319 (Sakai et al 1999); NGC 3351 (Graham et al 1997); NGC 3621 (Rawson et al 1997); NGC 4321 (Ferrarese et al 1996); NGC 4414 (Turner et al 1998); NGC 4535 (Macri et al 1999); NGC 4548 (Graham et al 1999); NGC 4725 (Gibson et al 1999b); NGC 5457 (Kelson et al 1996); NGC

7331 (Hughes et al 1998). Details about how the data was obtained and reduced can be found in these papers and the references therein.

The other 7 galaxies were from two sources: Tanvir et al (1995), Tanvir et al (1999) for NGC 3368 and the supernova calibration team of Sandage et al. (1996) for the galaxies NGC 3627, NGC 4639, NGC 4496A, NGC 4536, NGC 5253 and IC 4182. Once the data became available on the HST archive, the images for these galaxies were reanalysed by the Key Project team in Gibson et al (1999), using the same software and reduction procedure as for the other 18 galaxies. For consistency, the Cepheids in the HST images selected by Gibson et al (1999), along with their photometry and period determination are used here, rather than the originally published data.

3 P-L DISPERSION

Cepheid data was taken from the Key Project website and the references given in Section 2. An unweighted least squares fit was made to the magnitude versus period data for the Cepheids in each galaxy in both the V-band and the I-band. In this case, the line is the Cepheid P-L relation, which in the V-band is given by

$$m_V = -2.76 \log(P) - b \quad (1)$$

A similar relationship is used in the I-band with a P-L slope of -3.06 now assumed. The slope is held constant to that of the LMC P-L Relation (Madore and Freedman 1991). This is done to minimise the effects of magnitude limited bias, since this would tend to make the slope shallower. The Key Project team also follows this procedure in fitting their P-L Relations.

The mean r.m.s. dispersion about the P-L relation was also calculated, this is generally considered to be due to the small variation in magnitude across the instability strip and any statistical noise/experimental errors.

Plots of the P-L relations are given in Figure 1. The mean magnitude found from the Key Project photometry for each Cepheid is plotted against the period as calculated by the Key Project team. This is done in both the V- band and the I-band for all 25 galaxies. The plots show the best fitting line (solid black) to the data, along with the 2σ dispersion lines (dashed) for the LMC, within which most of the data should lie. Also shown are magnitude limits (horizontal broken lines). These were calculated from the exposure times given in the relevant papers (see section 2). The Key Project team do not calculate any magnitude limits, so we calculated consistent magnitude limits using the results of Tanvir et al (1999) as a basis. Here magnitude limits of 26 (in the V-band), and 25 (in the I-band), could be imposed. This, whilst somewhat arbitrary, is justified by Tanvir et al (1995), as the region where statistical noise starts to become significant. The magnitude limits are therefore not absolute limits of non-detection, and many of the P-L relations in Figure 1 contain Cepheids that lie below their respective magnitude limits. Table 2 lists the magnitude limits that have been calculated. The limits should be seen as the region where noise starts to become more significant and where there may be incompleteness in the number of Cepheids. The magnitude limits for the other galaxies were calculated by scaling the

exposure times (under the assumption that observing conditions are stable for the Hubble Space Telescope) relative to the exposure times given in Tanvir et al (1999), using signal-to-noise ratio considerations. However, at this stage the limits are not used in the calculation of the dispersion.

Also shown on the P-L plots in Figure 1, are possible limits in period for the P-L relations. This is due to the fact that short period Cepheids may not be detected in crowded stellar fields, since they are both dimmer and more difficult to identify as Cepheids. Using artificial star tests, Ferrarese et al (2000a), suggest that at Virgo and Fornax distances, P-L relations may be up to 50% incomplete below 20-25 days. They then applied period cuts at 20 and 25 days to all their P-L relations, and found a small increase in distance modulus for a small number of galaxies. Gibson et al (1999) report a similar effect for some of the non-Key Project galaxies. The P-L relation best fits, and hence distance moduli, were then revised, (by the Key Project team) for these galaxies. Following this, those galaxies recommended for period cuts by Ferrarese et al (2000a) and Gibson et al (1999) were re-examined by ourselves, and the same period cuts applied. Cepheids with periods below 20 days ($\log P = 1.3$) are not included in the best fit for the galaxies NGC 1326A, NGC 1425, NGC 4725, NGC 4536 and NGC 3368. Cuts at 25 days were done for NGC 1365, NGC 4535, NGC 4496A and NGC 3627. The intercept and dispersion shown on the P-L relations for these galaxies are for period cut samples.

Using these P-L relations, we then calculated distance moduli for the galaxies. This was done using data as used by the Key Project and ignoring our magnitude limits. The intercepts found from the best fit to the P-L relations were converted to V and I-band distance moduli using the LMC calibration of Madore and Freedman (1991). This was done by adding 1.4 to the V-band intercept and 1.81 to the I-band intercept (i.e. the galactic zero points from the LMC zero point of Madore and Freedman assuming an LMC distance modulus 18.5). The true distance modulus was then obtained using the following formula.

$$\mu_0 = \mu_{AV} - R(\mu_{AV} - \mu_{AI}) \quad (2)$$

where $R = 2.45$ after Cardelli et al (1989). The V-band modulus is simply corrected for absorption assuming a galactic reddening law.

Table 1 shows the parameters obtained from the P-L fits for each galaxy, (intercept and dispersion in the two wavebands, along with the calculated distance moduli and the distance in Mpc). The errors quoted on the distance moduli are from Ferrarese et al (2000a). The error has been split into random and systematic components. The random components are photometric errors, errors on the P-L fits and errors on the reddening correction. The error quoted is the random error. The systematic errors are the errors in the LMC calibration, the distance to the LMC, the photometry zero-point and metallicity differences. The systematic error would add a further ± 0.16 (in quadrature) to the error quoted in the Table. More details can be found in the relevant papers (see Section 2 for references).

Other parameters relevant to the galaxies are contained in Table 2. This includes the metallicity of the galaxy from HII regions in the region of the Cepheids used in the P-L relations (taken from Table 2 of Ferrarese et al (2000a) which is based on the references therein), and the mean

reddening (internal + galactic foreground), calculated from the Cepheids themselves. It is noted that Ferrarese et al (2000a) give the metallicity of NGC 3368 as $12 + \log[O/H] = 9.2 \pm 0.20$ based upon Oey and Kennicutt (1993). However Tanvir et al (1999) (and this paper) obtain 8.9 ± 0.1 based upon Oey and Kennicutt (1993). The value of 8.9 is therefore used in the rest of this paper. Also shown are the exposure times (from the references in Section 2) and magnitude limits calculated from these. The final column gives the number of Cepheids used in fitting the P-L relation.

Comparison with Published Distance Moduli

With one exception, the distance moduli calculated here (see Table 1) all agree with those published by the Key Project team (see Section 2 for references), to within 0.02 mag, and most agree exactly. The small discrepancies are thought to be due to simple rounding errors. The intercepts from the P-L relations usually agree and in the cases where they do not there is only a small change in distance modulus. The only exception was NGC 1326A. Here a distance modulus of 31.55 was obtained compared with 31.43 from Ferrarese et al (2000a). This is one of the galaxies that has had data cut at short period, and if all Cepheids are included a distance modulus of 31.36 is obtained, in agreement with Prosser et al (2000). After checking the right cuts have been made, there seems to be no explanation for the discrepancy between the value of 31.55 obtained here and the 31.43 obtained by Ferrarese et al (2000a). The value obtained here is used in the rest of this work.

So, using the same methods we confirm the Key Project results and in addition obtain the dispersion about the P-L relation (see Table 1).

4 RELATIONSHIP BETWEEN METALLICITY AND DISPERSION

One of the aims of this paper is to try and detect any signature of the effect of metallicity on Cepheids within a galaxy. In the first instance, our aim is to plot P-L dispersion against metallicity. The motivation is that high metallicity galaxies may have a wider intrinsic metallicity distribution than low metallicity galaxies and that this may result in a broader P-L relation for high metallicity galaxies.

4.1 V-Band Data

The V-band dispersion about the best fit to the P-L relation (Figure 1 and Table 1), was plotted against the metallicity (Table 2). The results are shown in Figure 2.

A least squares fit was performed on the data in Figure 2 as described in the previous section except the slope was not constrained to any particular value. A slope of $0.103 \pm 0.031 \text{ mag dex}^{-1}$ was obtained, which is significant at the 3.3σ level. The error is the standard error on the slope.

The least squares fit is unweighted as the errors on the metallicities and dispersions are comparable. The error bars are shown in Figure 3. One possible issue here is how the Cepheids are spatially distributed in the galaxies. Since there is a metallicity gradient in galaxies, Cepheids that are taken from a larger area of a galaxy should have a larger

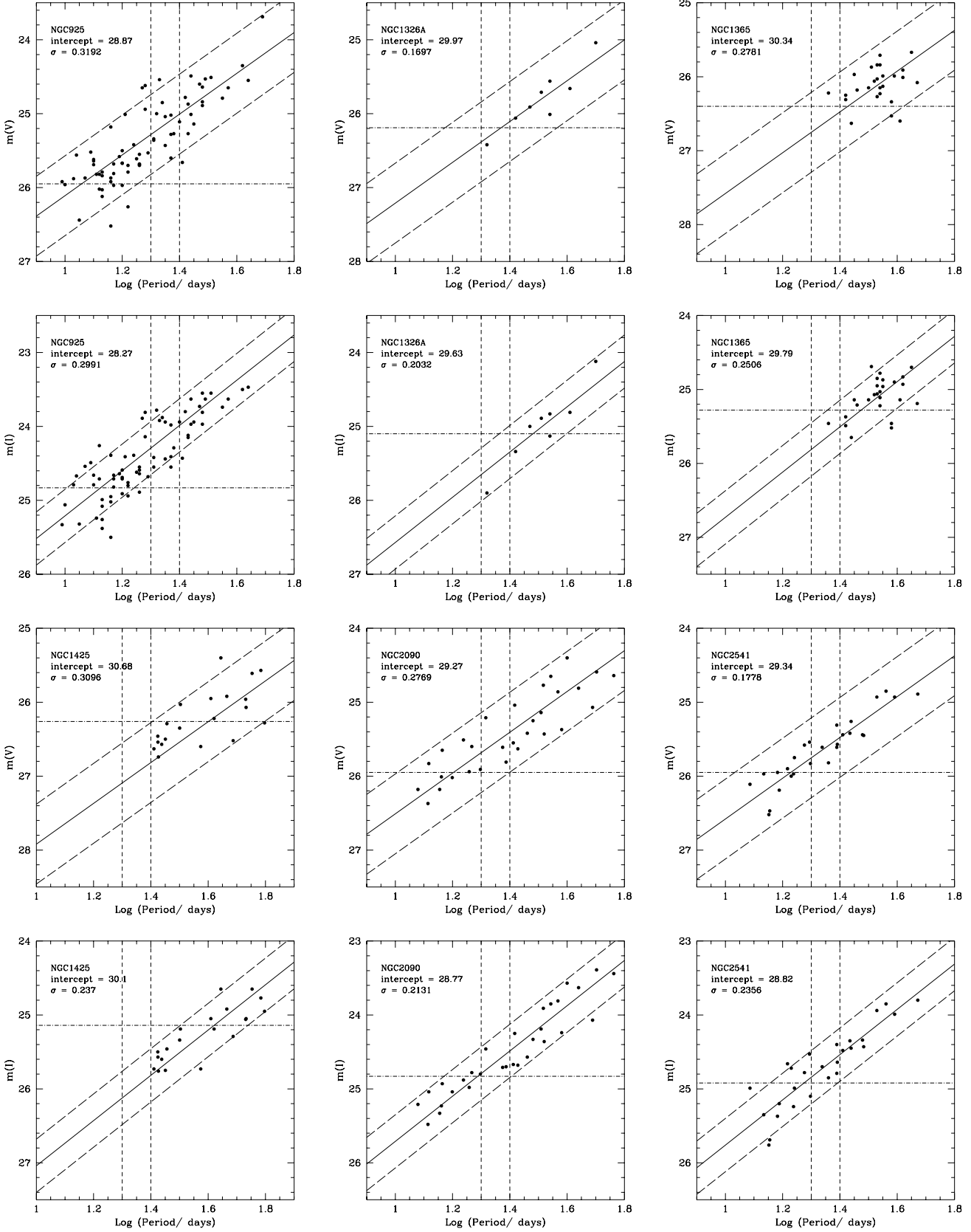


Figure 1. P-L Relation in V and I for 25 HST Cepheid Galaxies. The best fit to the data is shown as a solid black line along with 2σ LMC envelopes. Magnitude limits are shown as horizontal broken lines, and possible period limits are shown as vertical dashed lines *continued*.

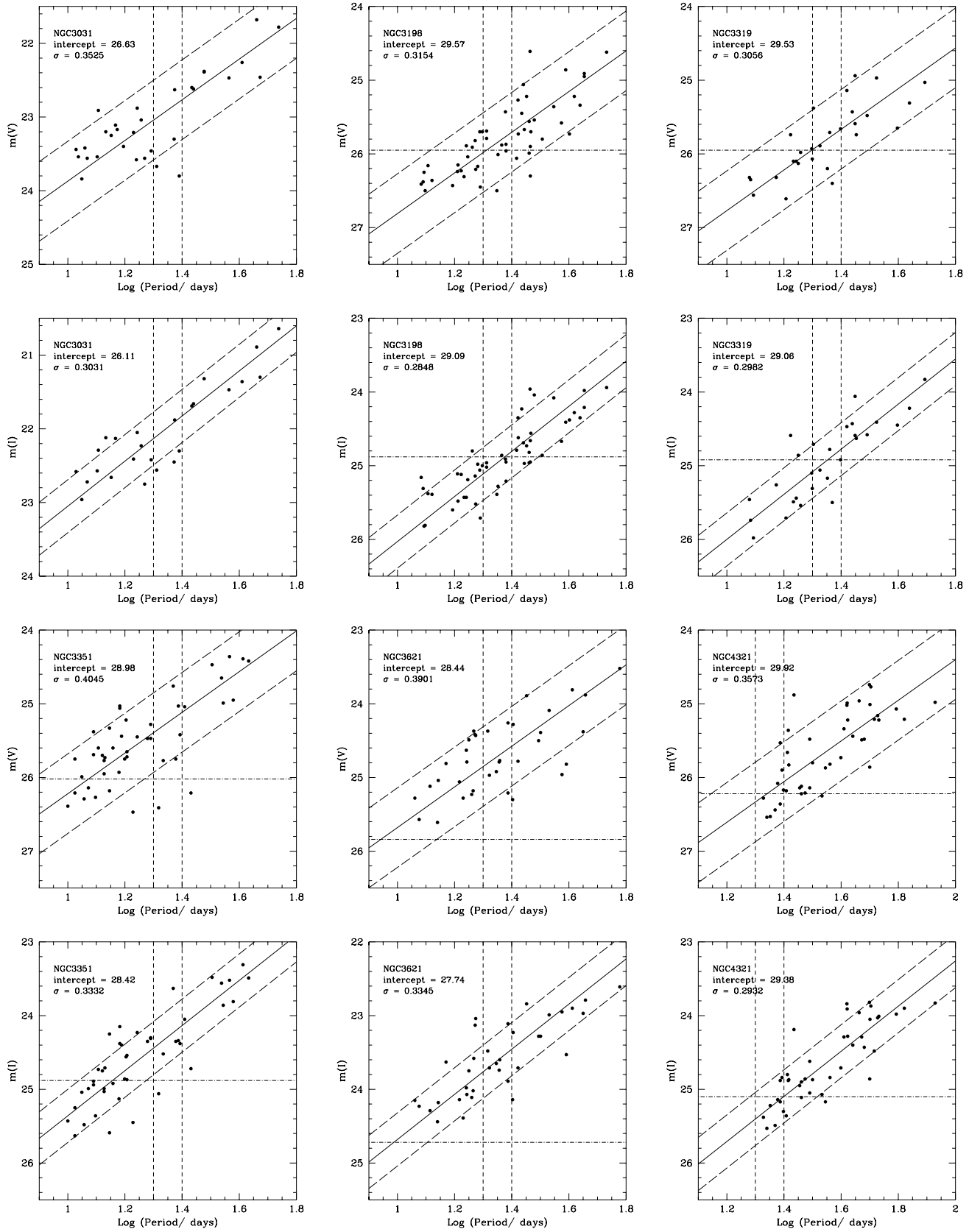


Figure 1. continued

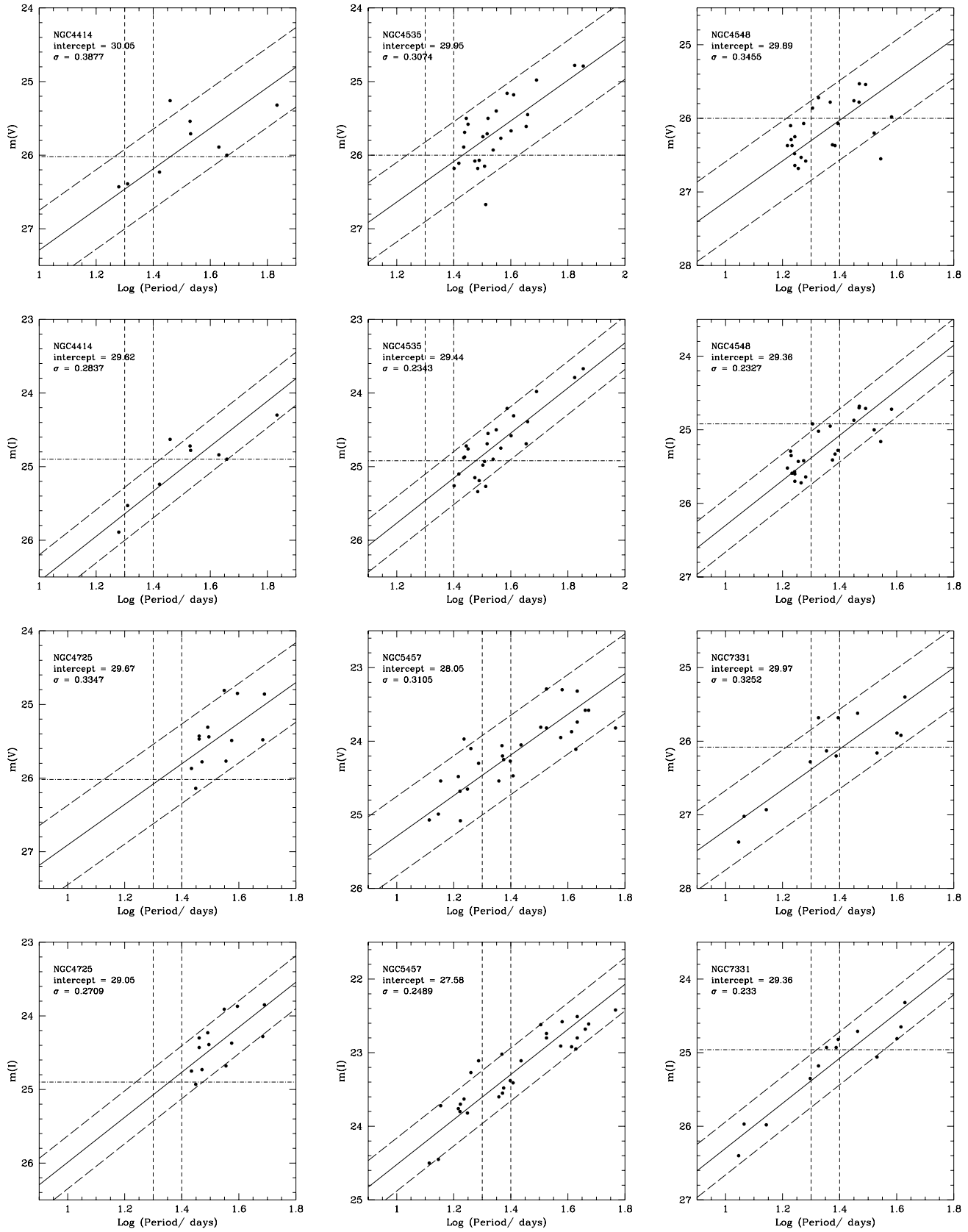


Figure 1. *continued*

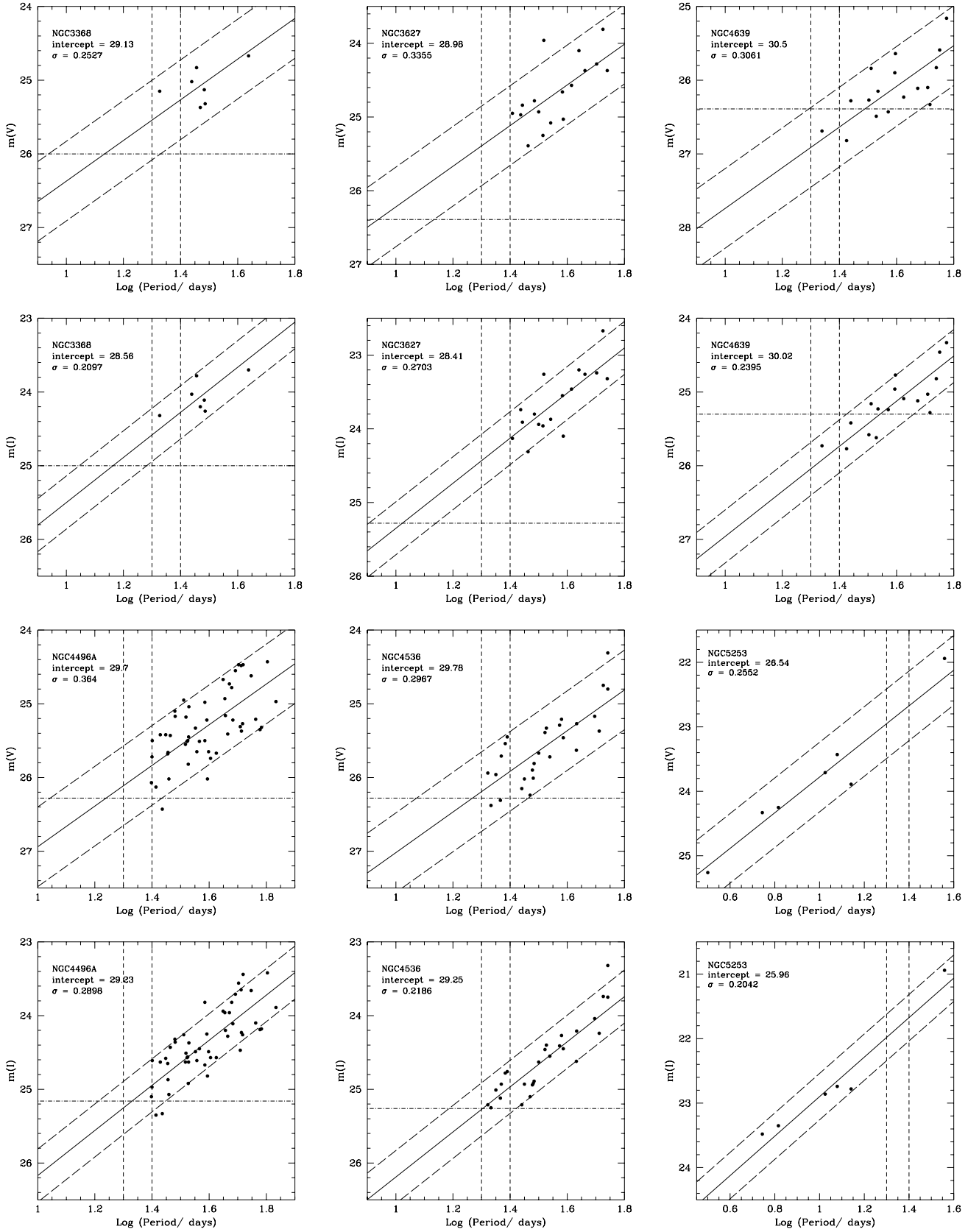


Figure 1. continued

Galaxy	Team	Intercept(V)	Dispersion(V)	Intercept(I)	Dispersion(I)	Distance Modulus	Distance (Mpc)
NGC 925	H ₀ Key Project	28.87	0.32	28.27	0.30	29.82 ± 0.08	9.29
NGC 1326A	H ₀ Key Project	29.97	0.17	29.63	0.20	31.55 ± 0.07	19.32
NGC 1365	H ₀ Key Project	30.34	0.28	29.79	0.25	31.40 ± 0.10	18.28
NGC 1425	H ₀ Key Project	30.58	0.31	30.10	0.24	31.82 ± 0.06	23.01
NGC 2090	H ₀ Key Project	29.28	0.28	28.77	0.21	30.45 ± 0.08	12.30
NGC 2541	H ₀ Key Project	29.34	0.18	28.82	0.24	30.46 ± 0.08	12.42
NGC 3031	H ₀ Key Project	26.63	0.35	26.11	0.30	27.77 ± 0.08	3.63
NGC 3198	H ₀ Key Project	29.57	0.32	29.09	0.28	30.80 ± 0.06	14.45
NGC 3319	H ₀ Key Project	29.53	0.31	29.06	0.30	30.78 ± 0.10	14.32
NGC 3351	H ₀ Key Project	28.98	0.40	28.42	0.33	30.01 ± 0.08	10.05
NGC 3621	H ₀ Key Project	28.44	0.39	27.74	0.33	29.14 ± 0.11	6.70
NGC 4321	H ₀ Key Project	29.92	0.36	29.38	0.29	31.04 ± 0.09	16.14
NGC 4414	H ₀ Key Project	30.05	0.39	29.62	0.28	31.41 ± 0.10	19.14
NGC 4535	H ₀ Key Project	29.95	0.31	29.44	0.23	31.11 ± 0.07	16.60
NGC 4548	H ₀ Key Project	29.89	0.35	29.36	0.23	31.01 ± 0.08	19.14
NGC 4725	H ₀ Key Project	29.67	0.33	29.05	0.27	30.56 ± 0.08	13.00
NGC 5457	H ₀ Key Project	28.05	0.31	27.58	0.25	29.34 ± 0.10	7.38
NGC 7331	H ₀ Key Project	29.97	0.33	29.36	0.23	30.90 ± 0.10	15.07
NGC 3368	Tanvir et al.	29.13	0.25	28.56	0.21	30.20 ± 0.10	11.59
NGC 3627	Sandage et al.	28.98	0.34	28.41	0.27	30.06 ± 0.17	11.07
NGC 4639	Sandage et al.	30.50	0.31	30.02	0.24	31.80 ± 0.09	25.47
NGC 4496A	Sandage et al.	29.70	0.36	29.23	0.29	31.02 ± 0.07	16.07
NGC 4536	Sandage et al.	29.78	0.30	29.25	0.22	30.95 ± 0.07	16.60
NGC 5253	Sandage et al.	26.54	0.26	25.96	0.20	27.61 ± 0.11	4.13
IC 4182	Sandage et al.	26.86	0.25	26.46	0.21	28.36 ± 0.08	4.70

Table 1. Data obtained from P-L fitting. Intercept and dispersion in each waveband, and the calculated distance modulus and distance

Galaxy	Reddening V-I	Metallicity 12 + Log(O/H)	Exposure (V) s	Exposure (I) s	m(V) limit	m(I) limit	Number of Cepheids
NGC 925	0.18 ± 0.03	8.55 ± 0.15	2200	2200	25.95	24.83	75
NGC 1326A	0.00 ± 0.01	8.50 ± 0.15	3400	3600	26.19	25.10	8
NGC 1365	0.20 ± 0.04	8.96 ± 0.20	5000	5000	26.40	25.28	26
NGC 1425	0.09 ± 0.04	9.00 ± 0.15	3900	3900	26.26	25.14	20
NGC 2090	0.09 ± 0.01	8.80 ± 0.15	2200	2200	25.95	24.83	30
NGC 2541	0.11 ± 0.07	8.50 ± 0.15	2200	2600	25.95	24.92	27
NGC 3031	0.04	8.75 ± 0.15	1200	1800	25.62	24.72	31
NGC 3198	0.07 ± 0.04	8.60 ± 0.15	2200	2400	25.95	24.88	52
NGC 3319	0.05 ± 0.04	8.38 ± 0.15	2200	2600	25.95	24.92	28
NGC 3351	0.15	9.24 ± 0.20	2500	2400	26.02	24.88	45
NGC 3621	0.30 ± 0.03	8.75 ± 0.15	1800	1800	25.84	24.72	36
NGC 4321	0.18 ± 0.11	9.13 ± 0.20	3600	3600	26.22	25.10	43
NGC 4414	0.01 ± 0.05	9.20 ± 0.15	2500	2500	26.02	24.90	9
NGC 4535	0.13 ± 0.04	9.20 ± 0.15	2400	2600	26.00	24.92	25
NGC 4548	0.12 ± 0.03	9.34 ± 0.15	2400	2600	26.00	24.92	24
NGC 4725	0.26 ± 0.04	8.92 ± 0.15	2500	2500	26.02	24.90	13
NGC 5457	0.18	9.05 ± 0.15	4200	4200	26.30	25.18	29
NGC 7331	0.19 ± 0.07	8.67 ± 0.15	2800	2800	26.08	24.96	13
NGC 3368	0.19 ± 0.05	8.90 ± 0.10	2400	3000	26.00	25.00	7
NGC 3627	0.19 ± 0.05	9.25 ± 0.20	4900	5000	26.39	25.28	17
NGC 4639	0.07 ± 0.04	9.00 ± 0.20	4900	5200	26.39	25.30	17
NGC 4496A	0.05 ± 0.03	8.77 ± 0.20	4000	4000	26.28	25.16	51
NGC 4536	0.13 ± 0.03	8.85 ± 0.20	4000	4000	26.28	25.16	27
NGC 5253	0.19 ± 0.07	8.15 ± 0.15	3600	3600	26.22	25.10	7
IC 4182	-0.04 ± 0.04	8.40 ± 0.20	4200	4200	26.30	25.18	28

Table 2. Some Cepheid galaxy parameters. Total mean reddenings for Cepheids in each galaxy, metallicity of region where Cepheids are found (from Ferrarese et al (2000a)), exposure times (from papers listed in section 2) along with calculated magnitude limits and the number of Cepheids used in fitting the P-L relation.

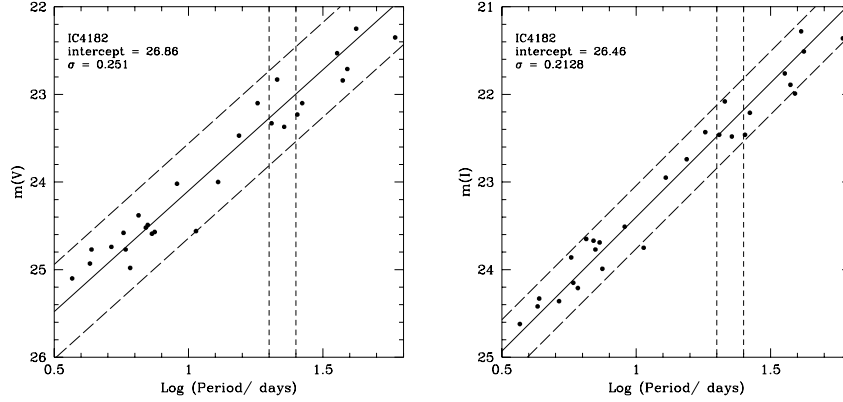


Figure 1. continued

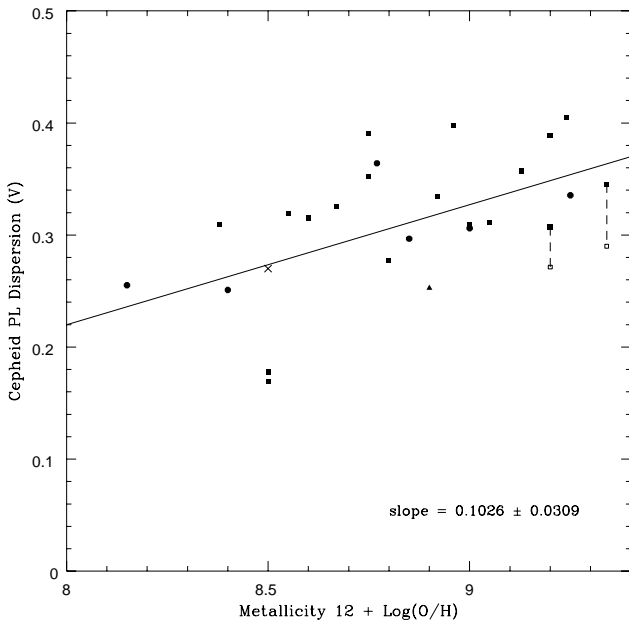


Figure 2. Relationship between mean r.m.s. dispersion (V-band) about the Cepheid P-L relation and metallicity of HII regions in the vicinity of the Cepheids. Data from the H₀ Key Project team is shown as squares. Sandage et al. data is shown as circles and the Tanvir et al data as a triangle (although in both these cases the Key Project photometry was used). Finally, the LMC is shown as a cross. The result of a least squares fit to the data is also shown.

dispersion. It is assumed here that the errors on the metallicities take this into account. Unfortunately it is not clear from Ferrarese et al (2000a) if this is the case, although it appears that measurement errors dominate in any case, so this effect is likely to be small.

An analysis of the P-L relations shows that two of the high dispersion/high metallicity galaxies contain outlying points. The galaxies are NGC 4535 and NGC 4548. The questionable points are shown as open squares rather than filled circles in the P-L relations in Figure 4. Consequently, the dispersion decreases for both the galaxies. NGC 4535 decreases from 0.3074 to 0.2714 and NGC 4548 from 0.3455 to 0.2900. On the dispersion/metallicity graph (Figure 2)

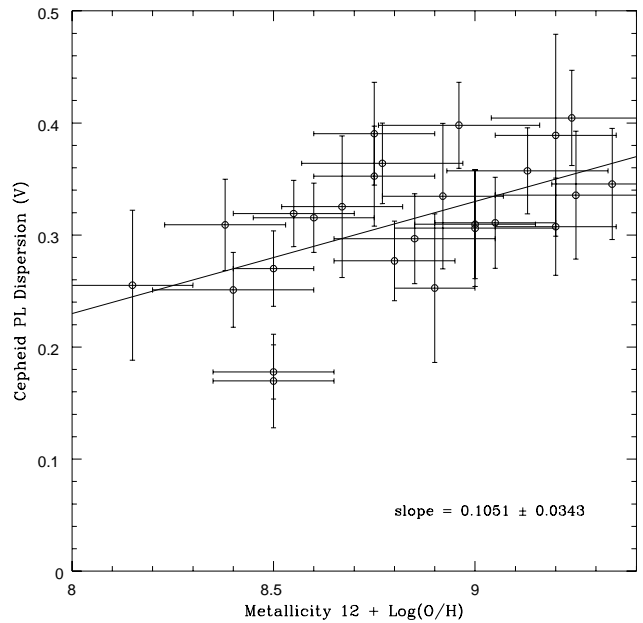


Figure 3. Relationship between mean r.m.s. dispersion (V-band) about the Cepheid P-L relation and metallicity of HII regions in the vicinity of the Cepheids, now showing the errors on both axes. The same unweighted least squares fit to the data is shown as in Fig. 2.

these alternative points are shown as open squares. Using these new points, a best fit to Figure 2 gives a slope of $0.085 \pm 0.033 \text{ mag dex}^{-1}$, which is significant at the 2.6σ level. The Key Project Team included these points in their work, and their Cepheid selection procedure is fairly conservative. It is unlikely that the points are not normal Cepheids, (they are also not outliers in the I-band data), and so they are included in this work, but the effect of their removal is noted.

There was some concern over incompleteness at short periods due to a magnitude limit or crowding at short periods. To investigate the effects of this, the data was cut in two ways. Using a cut in period at $P = 25$ days and a cut in period at the point where the lower LMC 2σ line crosses the magnitude limits calculated in Table 2. The results are shown for the V-band in Table 3. In many cases the num-

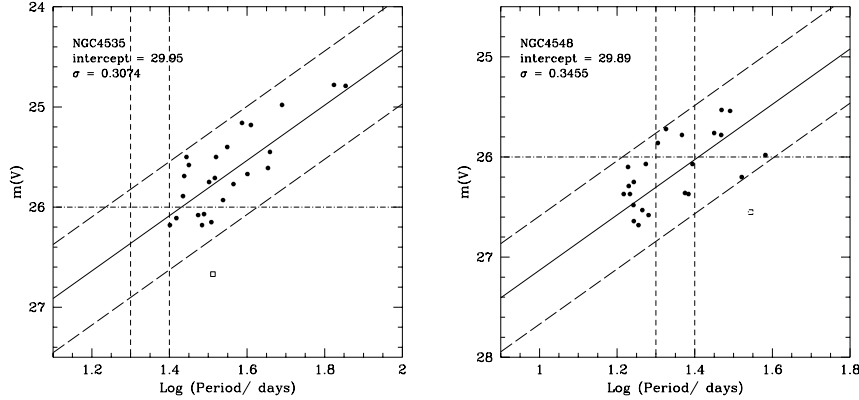


Figure 4. P-L (V) relations for NGC 4535 and NGC 4548. Each has a possible outlying point (shown as an empty square rather than a filled circle). This reduces the dispersion from 0.3074 to 0.2714, and from 0.3455 to 0.2900 respectively

ber of Cepheids that could be used in the P-L fit reduces dramatically.

A period cut at $P = 25$ days was applied to all the P-L relations. This either has little effect, or causes the number of Cepheids to be so small that the measured dispersion is not reliable. Also, the Key Project team (Ferrearese et al (1999)) has already examined the effects of cutting data at $P = 25$ days. We therefore revert to the Key Project recommendations for period cuts at $P = 25$ days (Ferrearese et al (2000a) and Gibson et al (1999)) in the rest of this paper.

Cuts in period where the lower LMC 2σ line crosses the magnitude limit can also mean that much of the data is lost, and in some cases it was not even possible to construct a P-L relation because only one Cepheid was left. In many cases there was also little change in dispersion or intercept. It was decided to consider changing those galaxies where there were 7 or more remaining Cepheids, and the dispersion had changed by more than 0.03 mag. Table 3 shows all these changes, with the last column showing the final selection.

Figure 5 shows the relationship between metallicity and data that has been selectively cut in period at the point where the 2σ LMC dispersion lines cross the magnitude limit. Cuts have been applied to NGC 925, NGC 1326A, NGC 3351, and NGC 4536. The best fit to the data is shown on the graph. A slope of 0.096 ± 0.030 is obtained which is still significant at the 3σ level. If the galaxies NGC 4535 and NGC 4548 have their dispersion changed due to outlying points, as described in the previous section, the slope reduces to 0.079 ± 0.033 mag dex $^{-1}$. This is significant at the 2.4σ level, and not much different than the value quoted in Figure 2.

Having considered the effects of systematically applying period cuts to the Cepheid data, we note that this can only be done in a small number of cases. It should also be noted that the changes to the metallicity/dispersion relation are small. For these reasons we use the original values based upon the Key Project period cutting recommendations given in Figure 1 in the rest of this paper.

Galaxy	Dispersion (published)	Dispersion P= 25 days	Dispersion P (mag)	Change y/n
NGC 925	0.32	0.37	0.33	y
NGC 1326A	0.17	0.18	0.26	y
NGC 1365	0.28	0.27	N/A	n
NGC 1425	0.31	0.31	N/A	n
NGC 2090	0.28	0.29	0.29	n
NGC 2541	0.18	0.15	0.16	n
NGC 3031	0.35	0.23	0.35	n
NGC 3198	0.32	0.38	0.29	n
NGC 3319	0.31	0.36	N/A	n
NGC 3351	0.40	0.47	0.45	y
NGC 3621	0.39	0.45	0.41	n
NGC 4321	0.36	0.38	0.36	n
NGC 4414	0.39	0.45	N/A	n
NGC 4535	0.31	0.31	N/A	n
NGC 4548	0.35	0.46	N/A	n
NGC 4725	0.33	0.33	N/A	n
NGC 5457	0.31	0.32	0.31	n
NGC 7331	0.33	0.38	0.35	n
NGC 3368	0.25	0.24	0.24	n
NGC 3627	0.34	0.34	0.34	n
NGC 4639	0.31	0.31	N/A	n
NGC 4496A	0.36	0.36	0.36	n
NGC 4536	0.30	0.28	0.26	y
NGC 5253	0.25	N/A	0.25	n
IC 4182	0.25	0.29	0.25	n

Table 3. V-band P-L relation dispersion using data as published and with period cut at $P = 25$ days and in period where the 2σ dispersion lines cross the magnitude limits

4.2 I-Band Data

As with the V-band data, the dispersions from Table 1 were plotted against the metallicities in Table 2. The result is shown in Figure 6. The best fit to this data gives a slope of 0.035 ± 0.026 . Although the relationship is in the same direction as the V-band data the result is less significant. It is therefore not possible to infer a relationship between the I-band dispersion and metallicity from this data.

The galaxies NGC 4535 and NGC 4548 do not have outlying points in the I-band data and so no attempt is made to recalculate their dispersions. Any magnitude cut

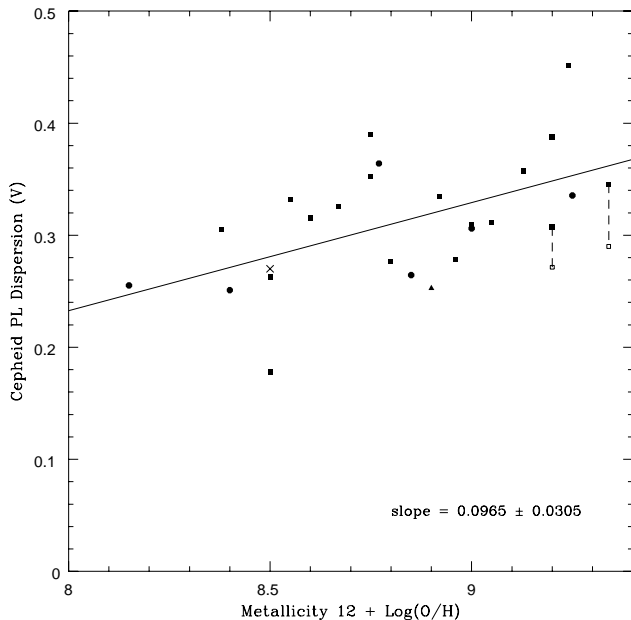


Figure 5. Relationship between mean r.m.s. dispersion (V-band) about the Cepheid P-L relation and metallicity of HII regions in the vicinity of the Cepheids. Magnitude cuts have been applied to data for the galaxies NGC 925, NGC 1326A, NGC 3351 and NGC 4536. Data from the H₀ Key Project team are shown as squares. Sandage et al data are shown as circles and the Tanvir et al data as a triangle (although in both these cases the Key Project photometry was used). Finally, the LMC is shown as a cross. The result of a least squares fit to the data is also shown.

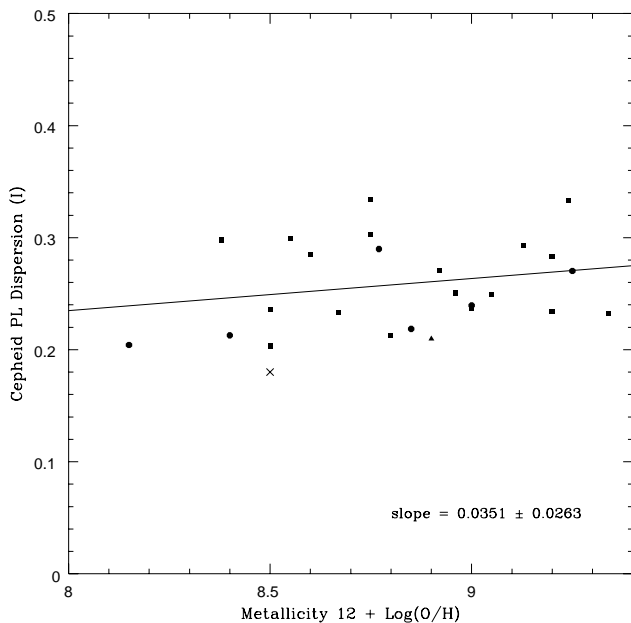


Figure 6. Relationship between mean r.m.s. dispersion (I-band) about the Cepheid P-L relation and metallicity of HII regions in the vicinity of the Cepheids. The same symbols are used as in Fig. 5. The result of a least squares fit to the data is also shown.

that could be made either leaves the dispersion unchanged (by more than 0.03 mag), or means that too much data is lost, and it is not possible to construct an accurate P-L relation.

4.3 Why is there a relationship in V but not in I?

One reason for expecting a relationship in I as well as V is that if Main Sequence fitted distance moduli to NGC7790 are overestimates due to low metallicity as claimed by Hoyle, Shanks & Tanvir (2001), then the effect of metallicity on Cepheid luminosity is expected to be broadly independent of passband. This is because a compensating and similar effect of metallicity on the three NGC7790 Cepheids is then required to maintain their tight position in the Galactic P-L relations from B through to K. Since a relationship between dispersion and metallicity can be inferred in V at the 3σ level but not in I, possible reasons for this result are now considered.

Reddening

Absorption due to dust is more significant in the V-band than the I-band. If a galaxy is particularly dusty (i.e. with a high reddening), then an uneven distribution of this dust would mean that the light from Cepheids is absorbed by differing amounts. In turn this could cause more variation in magnitude and so increase the dispersion about the P-L relation. Moreover, galaxies with high metallicity are more likely to be highly evolved and hence more dusty. This means that reddening due to absorption from dust could be the real cause of the relationship between metallicity and V-band dispersion. The relationship between reddening and metallicity is shown in Figure 7, which is an update of similar graphs in Kochanek (1997) and Kennicutt et al. (1998). The graph shows that again that there is a weak correlation between the amount of reddening toward a galaxy and the metallicities. The reddenings have the Galactic foreground reddening subtracted. The foreground reddenings were taken from the maps of Schlegel et al (1998) via the NASA/IPAC extragalactic database (NED) website (<http://nedwww.ipac.caltech.edu>).

The best fit to the unweighted points in Figure 7 gives a slope of $0.084 \pm 0.049 \text{ mag dex}^{-1}$. The significance level is 1.7σ , suggesting that reddening is unlikely to be the full cause of the observed relationship. Despite this, to fully verify that reddening does not cause the dispersion/ metallicity relationship, dispersion is plotted against metallicity in Figure 8 for those galaxies with low reddenings (i.e. $E_{V-I} < 0.13 \text{ mag}$). Here, the 10 most reddened galaxies are excluded from the sample of galaxies used in the fit to the dispersion/metallicity data. The dispersion data uses those galaxies with data cut due to possible magnitude incompleteness. The galaxies NGC 925, NGC 1365, NGC 3621, NGC 4321, NGC 4725, NGC 5457, NGC 7331, NGC 3368, NGC 3627 and NGC 5253 are excluded. A best fit to this data gives a slope of $0.13 \pm 0.040 \text{ mag dex}^{-1}$, a result significant at the 3σ level. Removal of outlier points in NGC 4535 and NGC 4548 (see Figure 4) reduces this slope to $0.10 \pm 0.049 \text{ mag dex}^{-1}$, which is significant at the 2σ level. Both these results are comparable to those obtained in the previous section. Removal of highly reddened galaxies has little

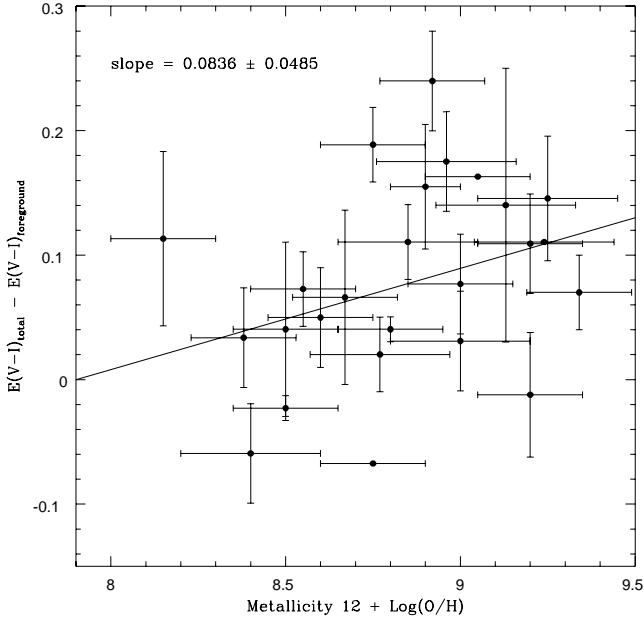


Figure 7. Relationship between metallicity and intrinsic reddening of the 25 HST Cepheid galaxies. The reddenings of the Cepheids have been corrected for galactic foreground reddening. The best fit to the data and its gradient is shown on the graph.

effect on the observed correlation and if anything makes the relationship slightly stronger, which again suggests that reddening is unlikely to be the cause of the relationship between V-band dispersion and metallicity.

Finally, in Figure 9, dispersion is plotted against reddening. No correlation is observed with a best fit to the data giving a slope of 0.083 ± 0.16 . On the basis of this data and these arguments it seems very unlikely that reddening is the cause of the high V-band dispersion at high metallicity.

Photometric Errors

The main possible causes of dispersion in the Cepheid P-L relation are variation in Cepheid temperature across the instability strip, reddening, metallicity and measurement errors, particularly in photometry. Unfortunately, photometry errors were only published for 15 of the galaxies, which are listed in Table 4. The photometry errors quoted by the Key Project team are very small (these were obtained from the relevant papers given in section 2) and are essentially based on epoch-epoch reproducibility for non-variable stars. In all cases the quoted I-band error is significantly larger than the V-band error (mean V-band photometry error = 0.045 mag c.f. mean I-band photometry error = 0.070mag). This is because the V-band light curves are constructed from observations at 12-15 epochs, whilst the I-band light curves are constructed from observations at 3-5 epochs. If the mean photometric errors are subtracted from the total dispersion in quadrature (see Table 4), then in both cases the mean change in dispersion is small. For the V-band this is 0.0049 mag, and for the I-band, 0.012 mag. These changes are shown in Table 4.

Since the change to the dispersion is small, little effect is made on the metallicity/dispersion relations, especially in

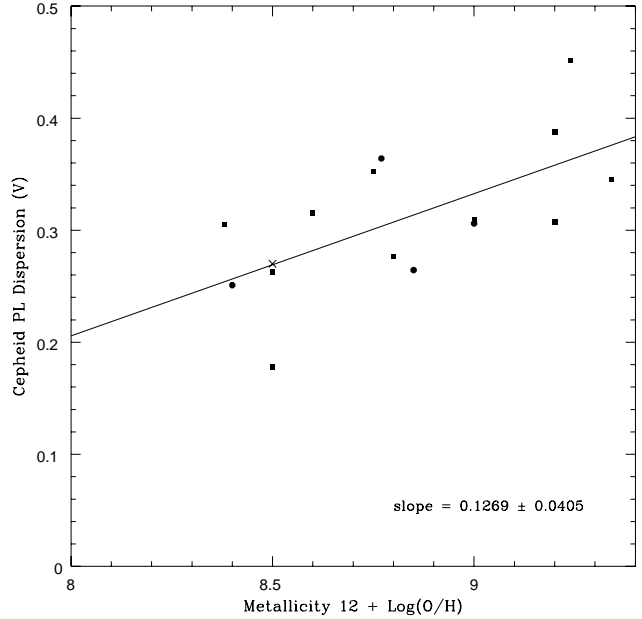


Figure 8. Relationship between mean r.m.s. dispersion (V-band) about the Cepheid P-L relation and metallicity of HII regions in the vicinity of the Cepheids, now using only the 10 least reddened galaxies. The same symbols are used as in Fig. 5. The result of a least squares fit to the data is also shown.

the V-band. The best fitting V-band slope is now $0.0750 \pm 0.035 \text{ mag dex}^{-1}$, which although significant at the 2σ level, is shallower and less significant than previous results. However, 10 data points are missing and these seem to be those galaxies with more extreme dispersions. It should also be noted that V-band photometry corrections make little difference to those points that have photometry errors available so it is very likely that this would also be the case for the remaining 10 points. It is therefore expected that photometry corrections would make little difference to the relationship between metallicity and V-band dispersion implied in this paper. In the I-band the changes are slightly more significant with the new best fitting slope $0.049 \pm 0.032 \text{ mag dex}^{-1}$. Although this is slightly steeper and more significant than Figure 6, it is still not possible to infer any relationship between metallicity and I-band dispersion. It appears that the photometric errors quoted by the KP are unlikely to have much effect on the measured dispersions about the P-L relations. They are small because they are based on observations at several epochs, even in the I-band.

Intrinsic Scatter

Intrinsic scatter in the P-L relation cause by Cepheid temperature differences at fixed period, which drive the Cepheid P-L-C relation, are significantly bigger than photometric errors. In the low-metallicity LMC, the intrinsic scatter in V is $\sigma_V = 0.27 \text{ mag}$ and in I it is $\sigma_I = 0.18 \text{ mag}$. From Figs. 2, 6 it is clear that intrinsic scatter plus photometric errors could plausibly dominate any metallicity induced P-L dispersion in HST galaxies at low metallicity ($12 + \log(O/H) \approx 8.5$). At high metallicity, ($12 + \log(O/H) \approx 9.4$), it is also clear that if the difference of $\sigma_{diff} = \sqrt{(0.27^2 - 0.18^2)} = 0.20 \text{ be}$

Galaxy	Photometry Error (V)	Photometry Error (I)	Corrected Dispersion (V)	Corrected Dispersion (I)	$\Delta\sigma(V)$	$\Delta\sigma(I)$
NGC 1365	0.10	0.11	0.26	0.22	0.020	0.026
NGC 3198	0.11	0.13	0.30	0.25	0.019	0.031
NGC 3368	0.031	0.037	0.25	0.21	0.0020	0.0033
NGC 3621	0.041	0.059	0.39	0.33	0.0022	0.0052
NGC 3627	0.025	0.033	0.33	0.27	0.0009	0.0020
IC 4182	0.018	0.098	0.25	0.19	0.0006	0.024
NGC 4414	0.040	0.069	0.39	0.28	0.0021	0.0085
NGC 4535	0.029	0.039	0.31	0.23	0.0014	0.0032
NGC 4536	0.026	0.041	0.30	0.21	0.0011	0.0038
NGC 4639	0.032	0.063	0.30	0.23	0.0017	0.0084
NGC 4725	0.024	0.041	0.33	0.27	0.0009	0.0031
NGC 5253	0.023	0.060	0.25	0.20	0.0010	0.0090
NGC 5457	0.090	0.11	0.30	0.23	0.013	0.024
NGC 7331	0.065	0.12	0.32	0.20	0.0066	0.035
NGC 4496A	0.020	0.039	0.36	0.29	0.0006	0.0027

Table 4. Columns 4,5 contain the dispersions corrected for the photometry errors given in Columns 2,3. The resulting differences in the dispersions are given in Columns 6,7.

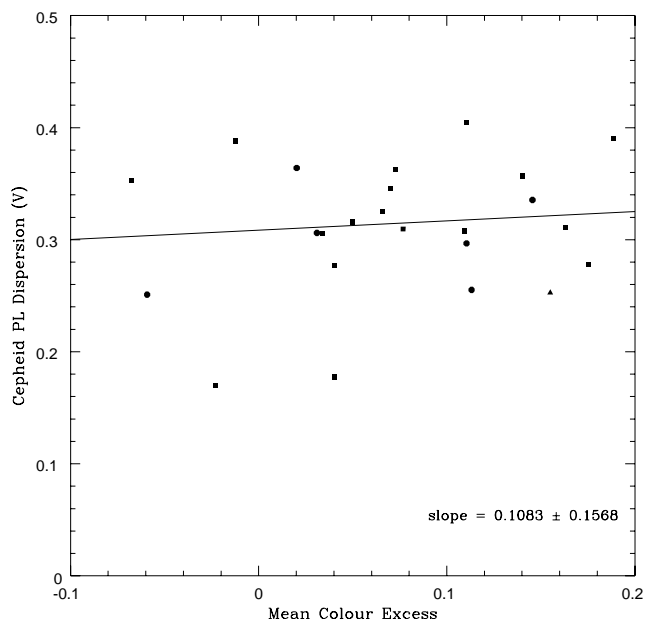


Figure 9. Relationship between mean r.m.s. dispersion (V-band) about the Cepheid P-L relation and mean colour excess of the Cepheids. The same symbols are used as in Fig. 5. The result of a least squares fit to the data is also shown.

tween the I and V band intrinsic dispersions is added to the observed HST I band dispersion of $\sigma_I \approx 0.28$ then a total dispersion of $\sigma_I = 0.34$ results, which is comparable to the observed $\sigma_V = 0.35$ at high metallicity in Fig. 2. Thus the data in Figs. 2, 6 at least at high metallicity is not inconsistent with the idea that the effect of metallicity on the P-L dispersions at I and V might be the same.

However, the dispersion in the lowest metallicity galaxies is similar in both I and V at $\approx \pm 0.25$ mag, so here there is no chance of arguing that the I dispersion drops with similar slope to low metallicity as in V, when the smaller I intrinsic dispersion is taken into account. Indeed, combining the LMC I dispersion of $\approx \pm 0.18$ and the average photo-

metric error in I of ± 0.07 mag only accounts for ± 0.19 mag, leaving a residual r.m.s. dispersion of ± 0.16 mag of the observed $\approx \pm 0.25$ mag. The same problem does not exist in the V band where the average of the low metallicity galaxies' dispersion is similar to that of the LMC (see Fig. 2). This makes it unlikely that the cause of the excess dispersion at low metallicity in I is reddening which would be expected to cause a bigger dispersion at V than in I.

Discussion

In the V-band it appears likely the observed increase in dispersion with metallicity is indeed caused by metallicity. Both reddening and photometry are likely to have little effect on this relationship. As pointed out in previous sections, there have been several recent empirical attempts to measure the effects of metallicity on Cepheids (Gould & Popowski (1997), Kennicutt et al. (1998), Hoyle, Shanks & Tanvir (2001)). These all seem to indicate that high metallicity Cepheids are brighter than low metallicity ones. A high metallicity galaxy is likely to be more highly evolved and complex, and therefore could contain Cepheids with varying metal content, including some low metallicity Cepheids. In a low metallicity, perhaps younger, galaxy, all the Cepheids are likely to be of low metallicity whereas in a high metallicity galaxy there is more likely to be a wider range of Cepheid metallicity and hence luminosity, causing increased dispersion about the P-L relation.

In the I-band there are a number of reasons why the dispersion-metallicity relation appears less strong. First, the effects of metallicity could be less significant in the I-band. This is suggested by Kennicutt et al. (1998) when referring to their version of Figure 7. However, as we have considered above it is also possible that because the I-band P-L relation is intrinsically tighter and the data more erroneous, the tight dispersion expected in the HST galaxy P-L relations at low metallicity may be masked by increased error. The difficulty for this explanation is that the quoted photometric errors are not enough to explain why the HST I dispersions are so much larger than the LMC dispersion. One possibility is that the effects of crowding are mostly neglected in

the KP estimate of the photometric error (as summarised in Table 4), which is essentially a measure of how well a magnitude reproduces epoch-epoch. The error caused by two unresolved stars being merged is not included in the above estimate. Using tests where artificial stars are added to real HST frames, Ferrarese et al (2000b) claim crowding does not systematically bias HST Cepheid photometry bright by more than 0.07mag and they use this to rebut claims of a larger effect by Mochejska et al (2000) and Saha et al (2000). However, Ferrarese et al (2000b) do not report the increased r.m.s. error caused by crowding. Also these authors sub-select the artificial stars that deviate by $> 3\sigma$ at one epoch against their mean over 4 epochs and this would seem to exclude the stars with crowding errors because here the underlying star will contribute at all epochs and so bias the mean magnitude. The fact that the HST P-L relations at LMC metallicity generally have significantly larger dispersions than observed in the LMC may thus argue that crowding makes a significant contribution of $\approx \pm 0.16\text{mag}$ in I to the real r.m.s. photometric error. In turn, this may also mean that the *systematic* error due to crowding is higher than claimed by Ferrarese et al (2000b) and closer to their average single frame offset for NGC1365 of $\approx 0.13\text{mag}$.

We conclude that a combination of crowding together with other smaller contributions from other effects such as reddening may increase the P-L dispersion and mask the existence of a similar metallicity-dispersion correlation in I as at V. Certainly, if the LMC dispersion is taken to be a more accurate measure of the I dispersion at low metallicity, the dispersion rises from ± 0.18 at $12 + \log(O/H) \approx 8.5$ to ± 0.25 at $12 + \log(O/H) \approx 9.4$ and this is of the same order as the differential effect of metallicity on the V dispersion.

5 CONSEQUENCES OF A RELATIONSHIP BETWEEN DISPERSION AND METALLICITY

5.1 Application of a Global Metallicity Correction

Several recent studies have attempted to measure the effects of metallicity on Cepheid magnitudes. Although there are now several authors claiming that high metallicity Cepheids are brighter than low metallicity ones e.g. Gould & Popowski (1997), Sasselov et al (1997), Kennicutt et al. (1998), Hoyle, Shanks & Tanvir (2001), the Key Project team do not yet apply any correction to their distances. This is because the errors associated with the metallicity correction are high and at best the relationships are significant at the 2σ level. For example, Kennicutt et al. (1998) measured $\Delta M/[O/H] \approx -0.24 \pm 0.16\text{mag}$ whereas Hoyle, Shanks & Tanvir (2001) claimed $\Delta M/[O/H] \approx -0.66$ which is only consistent with the relation of Kennicutt et al. (1998) at the 2.6σ level. However, this work, whilst not measuring the size of the global metallicity effect very accurately, does imply with a reasonable significance that Cepheid magnitudes are affected by metallicity.

In fact, if we take the observed error in the logarithmic metallicity of the highest metallicity galaxies' as $\approx \pm 0.2$ then the excess r.m.s. error in their V P-L dispersion of $\pm 0.25\text{mag}$ converts to $|\Delta M/[O/H]| \approx 0.25/0.2 \approx 1$. The excess in the I P-L dispersion for the high metallicity galaxies is smaller at $\pm 0.13\text{mag}$, converting to $|\Delta M/[O/H]| \approx$

$0.13/0.2 \approx 0.65$. Both these numbers are close to the claimed $\Delta M/[O/H] \approx -0.66$ metallicity correction of Hoyle, Shanks & Tanvir (2001). If the smaller $-0.24 \text{ mag dex}^{-1}$ of Kennicutt et al. (1998) applied, then the expected increase in dispersion is only $\pm 0.2 \times 0.24 \approx \pm 0.05\text{mag}$ which is too small to explain even the weaker I band correlation. We therefore take this as supporting evidence that a global metallicity correction should be applied to Cepheid distances. As a result of this, the effects of the $-0.66 \text{ mag dex}^{-1}$ metallicity correction of Hoyle, Shanks & Tanvir (2001) are now examined.

The Distance to the LMC

The distance to the LMC is likely to be one of the largest possible sources of systematic error in the Cepheid distance scale. One of the effects of applying a metallicity correction would be to reduce the Cepheid distance to the LMC, changing the zero point of the Cepheid P-L relation and cancelling the effect of the increased extragalactic distances. However, there is general disagreement between authors, over what the Cepheid distance to the LMC actually is (e.g. Hoyle, Shanks & Tanvir (2001) obtain a distance modulus of 18.5, whilst Feast and Catchpole (1997) obtain 18.7). Tanvir (1998) (after Madore and Freedman (1991)) cautions that it is perhaps unwise to rely on Cepheid distances alone for this step of the distance ladder, and recommends that a distance of 18.5 should be adopted as an average of different methods (Madore and Freedman 1991). These can include Cepheids, RR Lyrae and various techniques involving Supernova 1987A. As Tanvir (1998) points out, the Cepheid distances are generally on the high side in LMC distance determinations (i.e. > 18.5), and application of a metallicity correction may bring the Cepheid distances into line with those obtained using other methods.

Hoyle, Shanks & Tanvir (2001) obtain an LMC distance modulus of 18.5 ± 0.12 . Application of a metallicity correction to this (assuming $[O/H]$ for the LMC = -0.4) reduces the distance modulus to 18.24 ± 0.12 . However, this is clearly low compared with the independent distances obtained using RR Lyrae and SN1987A. It should also be noted that the distance modulus obtained by Hoyle, Shanks & Tanvir (2001) has a relatively large error associated with it. As a result of these uncertainties over the LMC distance the effects of a global metallicity correction are looked at in two different cases, taking the LMC absolute distance modulus to be 18.5 and 18.24, although 18.5 is the preferred distance modulus.

Cepheid Distances with a Global Metallicity Correction

The result of applying a $-0.66 \text{ mag dex}^{-1}$ metallicity correction is shown in Table 5, which list the modified distance moduli for LMC distance moduli of 18.5, and 18.24. The change to the published values is also noted along with their mean change. For LMC modulus = 18.24 there is little overall change (i.e. a mean of -0.039). However, for LMC modulus = 18.5, it can be seen that the published distances are too short by a mean value of 0.22 ± 0.17 , where the error estimate comes from the dispersion of the data. Whilst this result could have a significant effect, it should be noted that the error estimate is quite large.

Galaxy	Number of Cepheids	Distance Modulus (As Published)	Distance Modulus (Corrected) $\mu_{LMC} = 18.5$	$\Delta\mu$	Distance Modulus (Corrected) $\mu_{LMC} = 18.24$	$\Delta\mu$
NGC 925	75	29.82	29.85	0.03	29.59	-0.23
NGC 1326A	8	31.55	31.55	0	31.29	-0.26
NGC 1365	26	31.40	31.71	0.30	31.45	0.05
NGC 1425	20	31.82	32.15	0.33	31.89	0.07
NGC 2090	30	30.45	30.65	0.20	30.39	-0.06
NGC 2541	27	30.46	30.46	0	30.20	-0.26
NGC 3031	25	27.77	27.94	0.17	27.68	-0.09
NGC 3198	52	30.80	30.87	0.07	30.61	-0.19
NGC 3319	28	30.78	30.70	-0.08	30.44	-0.34
NGC 3351	45	30.01	30.50	0.49	30.24	0.23
NGC 3627	36	29.14	29.30	0.16	29.04	-0.10
NGC 4321	43	31.04	31.46	0.42	31.20	0.16
NGC 4414	9	31.41	31.87	0.46	31.61	0.20
NGC 4535	25	31.11	31.57	0.46	31.31	0.20
NGC 4548	24	31.01	31.56	0.55	31.30	0.29
NGC 4725	13	30.56	30.84	0.28	30.58	0.02
NGC 5457	29	29.34	29.70	0.36	29.44	0.10
NGC 7331	13	30.90	31.01	0.11	30.75	-0.15
NGC 3368	7	30.20	30.47	0.27	30.21	0.01
NGC 3627	17	30.06	30.56	0.50	30.30	0.24
NGC 4639	17	31.80	32.13	0.33	31.87	0.07
NGC 4496A	51	31.02	31.20	0.18	30.94	-0.08
NGC 4536	27	30.95	31.18	0.23	30.92	-0.03
NGC 5253	7	27.61	27.38	-0.23	27.12	-0.49
IC 4182	28	28.36	28.30	-0.06	28.04	-0.32

Table 5. The effects of metallicity on Cepheid distances and the change in distance, taking absolute distance moduli $\mu_{LMC} = 18.50$ and $\mu_{LMC} = 18.24$.

The relationship between published Cepheid distance and corrected Cepheid distance is shown in Figure 10. It can be seen here more clearly that most of the original distances are too short. The black line is the line of equal distances and most of the points lie below this line.

5.2 Bias due to incompleteness at faint magnitudes

There is another consequence of the observed relationship between dispersion and metallicity. An increase in dispersion means that any bias due to incompleteness at faint magnitudes that is present, would become more significant. The implication is that high metallicity galaxies could be even further away than they are with just a global metallicity correction applied, because their distances are also biased too short. Of course, even if there were no relation with metallicity, the bigger than expected P-L dispersions observed in the HST sample would still produce a bias towards distances which are too low.

There are two ways to deal with this problem. The first method is to only use data in regions of the P-L relation where there is confidence that most of the data is above the magnitude limit. The best way of doing this is by calculating the period where the 2σ dispersion lines cross the magnitude limit, and then cutting all data with *periods* less than this value. This technique has already been used to check the effects of magnitude incompleteness on dispersion in section 4.1. However, this method is fairly unsatisfactory for what is required here (i.e. accurate distance determination). This

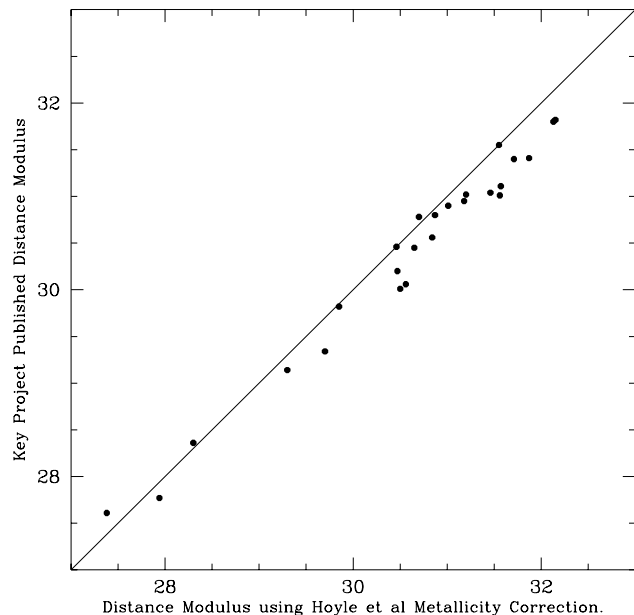


Figure 10. Relationship between published Cepheid distance modulus and metallicity corrected distance modulus. The solid line shows the line of equal distances. It can be seen that the published distances are generally shorter than the corrected ones. This assumes an absolute distance modulus of $\mu_{LMC} = 18.50$.

is because except in the small number of cases where the data is well clear of the magnitude limit (and no data has to be cut), the cuts applied are usually too drastic. In many cases the range in period left to use in the P-L relation is less than 0.3 (log (days)). The number of remaining Cepheids is also usually very small. This means that the accuracy of the distances obtained is questionable. After analysing the V-band data, it was decided that this method was unsuitable.

The Maximum Likelihood Method

The other way to calculate distances under a possible (magnitude limited) incompleteness bias is to use a maximum likelihood technique. We assume that the probability of a point being a certain distance from the line is given by a Gaussian, with the added restriction that the probability that a point exists below the magnitude limit is zero. The Gaussian must therefore be normalised to account for this. For the V-band this is

$$p_i = \frac{\exp\left(\frac{-(m_i - 2.76 \text{Log} p_i + a)}{2\sigma^2}\right)}{\int_{m_0}^{\infty} \exp\left(\frac{-(m_i - 2.76 \text{Log} p_i + a)}{2\sigma^2}\right)} \quad (3)$$

where p_i is the probability, m_i the magnitude, σ the dispersion, a the intercept and m_0 is the calculated magnitude limit.

The total probability for the whole data set is simply a product of these probabilities.

$$p = \prod_i p_i(a) \quad (4)$$

This is usually converted to a logarithm so that the product symbol can be exchanged for a summation.

$$\text{Log} p = \sum_i \text{Log} p_i(a) \quad (5)$$

This likelihood can be calculated using all data points that lie above the magnitude limit, with no restriction on period. The value of the intercept, a , which maximises this function can then be found. The number of points lost using this technique is minimised and the range in period available for the P-L relation is not greatly restricted. The maximum likelihood technique therefore allows distances to be determined accounting for magnitude limits.

The maximum likelihood intercept for all 25 galaxies in both V and I bands was calculated using a FORTRAN programme written to find the value of the intercept, a , which maximises equation 5. From these intercepts new distances were calculated and these are shown in Table 6.

Table 6 shows that in general, the distance moduli are increased by a small amount after maximum likelihood fitting. An average increase of $0.085 \pm 0.03 \text{mag}$ is obtained, although many of the values are close to zero. Plotting maximum likelihood distance against the previous distances (Figure 11) reveals that most of the significant differences are at large distances. This is likely to be because these are the furthest galaxies, and so more prone to magnitude incompleteness and bias.

Galaxy	μ_0 (as published)	μ_0 (maximum likelihood)	$\Delta\mu_0$
NGC 925	29.82	29.88	0.06
NGC 1326A	31.55	31.42	-0.13
NGC 1365	31.40	31.48	0.08
NGC 1425	31.82	32.22	0.40
NGC 2090	30.45	30.52	0.07
NGC 2541	30.46	30.48	0.02
NGC 3031	27.77	27.77	0.00
NGC 3198	30.80	30.93	0.13
NGC 3319	30.78	30.80	0.02
NGC 3351	30.01	29.95	-0.06
NGC 3621	29.14	29.15	0.01
NGC 4321	31.04	31.03	-0.01
NGC 4414	31.41	31.99	0.58
NGC 4535	31.11	31.18	0.07
NGC 4548	31.01	31.24	0.23
NGC 4725	30.56	30.56	0.00
NGC 5457	29.34	29.35	0.01
NGC 7331	30.90	31.28	0.38
NGC 3368	30.20	30.21	0.01
NGC 3627	30.06	30.06	0.00
NGC 4639	31.80	31.92	0.12
NGC 4496A	31.02	31.02	0.00
NGC 4536	30.95	31.08	0.13
NGC 5253	27.61	27.61	0.00
IC 4182	28.36	28.36	0.00

Table 6. Published distance moduli and distance moduli using maximum likelihood method.

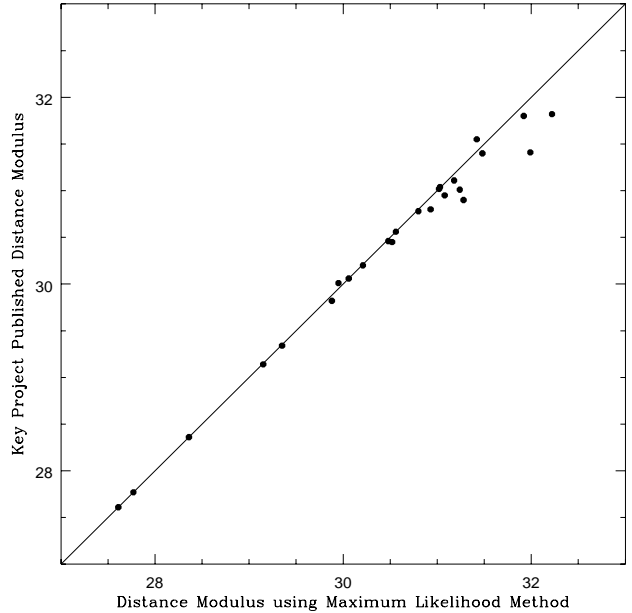


Figure 11. Relationship between published Cepheid distance modulus and distance modulus using maximum likelihood method. The solid line shows the line of equal distances.

Galaxy	KP (as pub.)	Hoyle	ML	ML +Hoyle	ML (mean disp.)
NGC925	29.82	29.85	29.88	29.91	29.81
NGC1326A	31.55	31.55	31.42	31.42	31.44
NGC1365	31.40	31.71	31.48	31.79	31.45
NGC1425	31.82	32.15	32.22	32.55	32.32
NGC2090	30.45	30.65	30.52	30.72	30.53
NGC2541	30.46	30.46	30.48	30.48	30.39
NGC3031	27.77	27.94	27.77	27.94	27.77
NGC3198	30.80	30.87	30.93	31.00	30.96
NGC3319	30.78	30.70	30.80	30.72	30.73
NGC3351	30.01	30.50	29.95	30.44	29.94
NGC3621	29.14	29.30	29.15	29.31	29.14
NGC4321	31.04	31.46	31.03	31.45	31.03
NGC4414	31.41	31.87	31.99	32.45	32.04
NGC4535	31.11	31.57	31.18	31.64	31.21
NGC4548	31.01	31.56	31.24	31.79	31.55
NGC4725	30.56	30.84	30.56	30.84	30.57
NGC5457	29.34	29.70	29.35	29.71	29.35
NGC7331	30.90	31.01	31.28	31.39	31.41
NGC3368	30.20	30.47	30.21	30.48	30.22
NGC3627	30.06	30.56	30.06	30.56	30.06
NGC4639	31.80	32.13	31.92	32.25	31.95
NGC4496a	31.02	31.20	31.02	31.20	31.01
NGC4536	30.95	31.18	31.08	31.31	31.11
NGC5253	27.61	27.38	27.61	27.38	27.61
NGC4182	28.36	28.30	28.36	28.30	28.36

Table 7. Distance moduli as published by Key Project (2), corrected for global metallicity correction of Hoyle et al. (2000) (3), using maximum likelihood method (4), combined maximum likelihood and global correction (5) and just maximum likelihood with no metallicity correction (6).

5.3 Total Metallicity Effects

The maximum effect of the Hoyle, Shanks & Tanvir (2001) global metallicity correction (i.e. taking LMC modulus = 18.5) and the magnitude incompleteness (maximum likelihood) effect are combined in Table 7 and Figure 12. The mean difference in distance modulus between metallicity corrected and non-metallicity corrected data, is now 0.31 ± 0.06 mag. There is also some evidence here of a scale error. The best fit to the data gives a slope of 0.085 ± 0.036 , differing from unity by 4.2σ . In the HST sample, there is a tendency for the highest redshift galaxies to be brighter and have high metallicity and the combined effect of the resulting high P-L dispersion and the global metallicity correction, means that there is a scale error, rather than just a simple offset, between the corrected and uncorrected distances.

6 POTENTIAL IMPLICATIONS FOR THE DISTANCE SCALE

The dispersion-metallicity correlation supports the idea that the metallicity dependence of Cepheid luminosities may be stronger than expected and is consistent with the $\frac{\Delta M}{[O/H]} = -0.66$ coefficient for the effect on the P-L relation suggested by Hoyle, Shanks & Tanvir (2001). Further, the increased dispersion observed in HST Cepheid galaxy P-L relations over that seen in the LMC suggests that the effects of magnitude incompleteness is larger than expected, particularly for the most distant galaxies. This latter effect would be

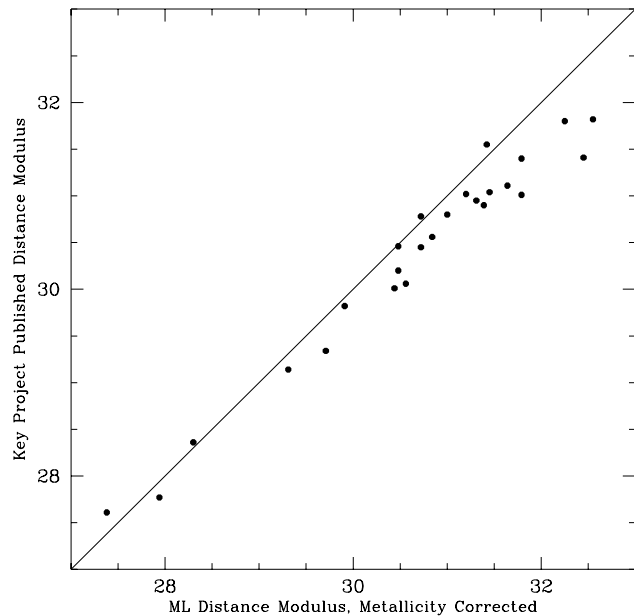


Figure 12. Relationship between published Cepheid distance modulus and distance modulus using maximum likelihood method and the Hoyle et al. metallicity correction. The solid line shows the line of equal distances.

present even if there is assumed to be no relation between P-L dispersion and metallicity, since the HST Cepheid P-L relations have a much higher dispersion than the LMC P-L relations.

6.1 Corrected distances to the Virgo, Fornax and Leo Galaxy Clusters

We first illustrate the possible effect on the distance scale and Hubble's Constant by comparing the new metallicity corrected average of the four galaxies in the Virgo cluster core, defined as within a radius of 6 degrees of M87 (NGC4321, NGC4414, NGC4535, NGC4548) with the published average (from Table 7, cols. 2, 5). The Virgo distance modulus increases from $(m - M)_0 = 31.24 \pm 0.19$ to $(m - M)_0 = 31.78 \pm 0.17$ or from 17.7 ± 1.6 Mpc to 22.7 ± 1.8 Mpc. Including the further two galaxies which are within a radius of 10 degrees of M87, NGC4496A and NGC4536, the Virgo distance modulus now increases from $(m - M)_0 = 31.15 \pm 0.13$ to $(m - M)_0 = 31.61 \pm 0.16$ or from 17.0 ± 1.0 Mpc to 21.0 ± 1.6 Mpc. The errors in the Virgo distance are large because the Virgo spirals are thought to have significant line-of-sight depth as evidence by their almost flat velocity distribution. Below we shall use corrected TF distances to obtain an alternative estimate of the Virgo distance which is based on more Virgo spirals. The Leo distance modulus increases from 30.09 ± 0.06 to 30.49 ± 0.04 or from 10.4 ± 0.3 Mpc to 12.5 ± 0.3 Mpc based on the 3 galaxies NGC3351, NGC3368 and NGC3627. The Fornax distance modulus increases from 31.59 ± 0.12 to 31.92 ± 0.33 or from 20.8 ± 1.2 Mpc to 24.2 ± 4.0 Mpc based on the galaxies NGC1326a, NGC1365 and NGC1425. The Fornax cluster forms the Eastern wall of the Sculptor Void and the dispersion in the Fornax spirals may be expected to be large

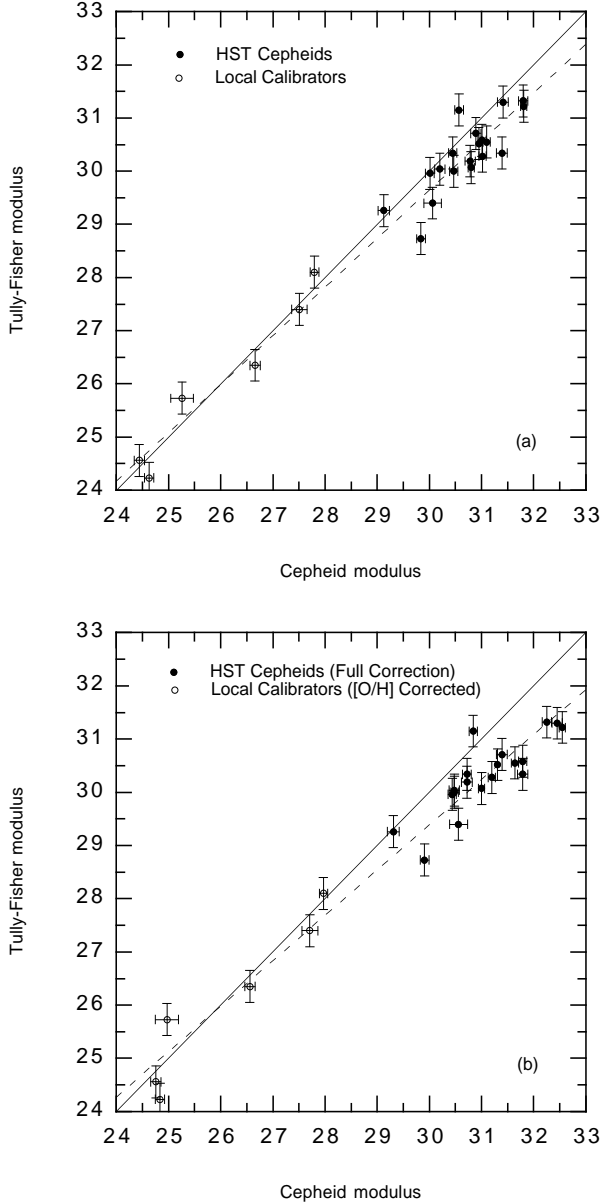


Figure 13. (a) A comparison between HST Cepheid and TF distances which suggests that TF distances show a significant scale-error with the TF distance to galaxies at the distance of the Virgo cluster being underestimated by $22 \pm 5.2\%$. The solid line shows the best fit with $(m - M)_{TF} = 0.915 \pm 0.036 \times (m - M)_{Ceph} + 2.204$. (b) The same as (a) with the Cepheid distances now having been fully corrected for metallicity from Table 7. An even stronger scale error is now seen, with the TF distances to galaxies at the distance of the Virgo cluster now shown to be underestimates by $46 \pm 6.7\%$. The solid line shows the best fit with $(m - M)_{TF} = 0.85 \pm 0.036 \times (m - M)_{Ceph} + 3.847$.

(Ratcliffe et al 1996). As for Virgo, below we shall therefore also use corrected TF distances to obtain an alternative estimate of the Fornax distance based on 21 Fornax spirals.

6.2 New Tests of Tully-Fisher Distances

We next illustrate the possible effect on the distance scale and Hubble's Constant by using the example of the Tully-

Fisher relation, since a significant number of the HST Cepheid galaxies have Tully-Fisher distances. In Figure 13(a) we therefore show the comparison of I-band Tully-Fisher distances, calculated on the same premises as Pierce & Tully (1992) and with our assumed TF parameters given in Table 8, with the published KP Cepheid distances from Table 7. Note that the average difference between our I_T magnitudes and those published by Macri et al (2000) is only on average 0.03 ± 0.04 mag. Also shown are the previous 6 local TF calibrators, M31, M33, M81, NGC2403, NGC300, NGC3109. This is similar to Fig. 2 of Shanks (1999), updated from the 13 HST Cepheid/TF galaxies available then to the 19 such galaxies available now, taking a lower limit for galaxy inclination of $i > 35$ deg. For the 18 HST Cepheid galaxies beyond $(m-M)_0 > 29.5$, we find that the TF distance moduli underestimate the Cepheid distance moduli by 0.44 ± 0.093 mag, a 4.7σ effect. Thus TF distances are confirmed to have been underestimated by $22 \pm 5\%$. Fitting a least squares line to all the galaxies in Figure 13(a) gives a slope of 0.915 ± 0.036 which is 2.4σ evidence that it is a real scale-error rather than a simple off-set causing the effect.

In Figure 14(a) we show the Cepheid-TF distance modulus residuals plotted against galaxy linewidth. The 19 HST Cepheid galaxies show a 2σ correlation in the sense that the lower linewidth, lower luminosity galaxies are fainter. Shanks (1999) previously suggested this was a possible signature of Malmquist bias (see Sandage (1994)) in the TF relation. The Local Calibrators in Figure 14(a) show the same slope but at approximately zero offset.

Now in Fig. 13(b) we show the same TF galaxy data as in Figure 13(a) but with Cepheid moduli now fully corrected for metallicity in the case of the HST galaxies (i.e. from col. 5 of Table 7) and in the case of the Local Calibrators just for the global metallicity correction (i.e. from col. 8 of Table 9). Note that in both cases this means we have normalised the metallicity to the LMC value of $12 + \log[O/H] = 8.5$ rather than the Galactic value of $12 + \log[O/H] = 8.9$, effectively assuming that the LMC distance is known independently of the Cepheids. The Local Calibrators overall have a slightly smaller average Cepheid distance because of the metallicity corrections, with the Cepheid-TF distance modulus difference moving to 0.073 ± 0.19 from -0.01 ± 0.14 ; this is principally due to the low metallicities of NGC3109 and NGC300. It should also be noted that the TF linewidth of NGC3109 is uniquely small at $\log W^R_I = 2.032$ (see Figure 15) and therefore the TF distance may be unreliable. The previously published Cepheid distance to this galaxy is also the subject of discussion (Ferrarese et al 2000a, Musella et al 1998).

For the HST Cepheid galaxies, it can be seen that TF distances beyond distance modulus $(m-M)_0 = 29.5$ are now found to underestimate the HST Cepheid distance moduli by 0.82 ± 0.10 mag or by $46 \pm 6.7\%$ in distance. The least squares fit to the TF:Cepheid data shown as the dashed line in Fig. 13(b) has slope 0.85 ± 0.036 which represents 4.2σ evidence for a scale error in the TF distances rather than a simple offset.

In Fig. 14(b) we show the residual-linewidth plot as in Fig. 14(a) but for the corrected Cepheid data. The metallicity corrections have left the low linewidth points approximately unchanged in this diagram but have made the residuals for the higher linewidth points bigger and compar-

Name	TF Distance	Inc	$\log W^R_I$	I_T	I_{corr}	$B - I_{corr}$	KP	Corrected	KP-TF	Corr-TF
NGC0925	28.73±0.3 ¹	57.0	2.349	9.30	9.11	1.34	29.84±0.08	29.91	1.11	1.18
NGC1365	30.34±0.3 ³	57.0	2.634	8.31	8.23	1.91	31.39±0.10	31.79	1.05	1.45
NGC1425	31.22±0.3 ³	63.5	2.566	9.82	9.70	1.32	31.81±0.06	32.55	0.59	1.33
NGC2090	30.34±0.3 ⁵	61.0	2.475	9.72	9.62	2.14	30.45±0.08	30.72	0.11	0.38
NGC2541	30.00±0.3 ⁷	59.9	2.296	11.02	10.84	1.02	30.47±0.08	30.48	0.47	0.48
NGC3198	30.07±0.3 ⁷	67.1	2.484	9.41	9.27	1.28	30.80±0.06	31.00	0.73	0.93
NGC3319	30.19±0.3 ⁶	56.7	2.348	10.66	10.58	0.72	30.78±0.10	30.72	0.59	0.53
NGC3351	29.96±0.3 ²	47.5	2.511	-	8.92	1.45	30.01±0.08	30.44	0.05	0.48
NGC3368	30.04±0.3 ²	46.2	2.641	-	7.88	2.08	30.20±0.10	30.48	0.16	0.44
NGC3621	29.26±0.3 ⁴	54.9	2.471	8.83	8.57	1.12	29.13±0.11	29.31	-0.13	0.05
NGC3627	29.40±0.3 ¹	58.0	2.603	7.67	7.56	1.77	30.06±0.17	30.56	0.66	1.16
NGC4414	31.30±0.3 ¹	50.0	2.696	-	-	-	31.41±0.10	32.45	0.11	1.15
NGC4496a	30.28±0.3 ¹	43.0	2.328	10.88	10.84	1.47	31.02±0.07	31.20	0.74	0.92
NGC4535	30.55±0.3 ⁷	44.9	2.559	9.13	9.09	1.41	31.10±0.07	31.64	0.55	1.09
NGC4536	30.52±0.3 ¹	70.0	2.525	9.53	9.36	1.69	30.95±0.07	31.31	0.43	0.79
NGC4548	30.58±0.3 ⁷	37.4	2.586	8.95	8.89	1.94	31.01±0.08	31.79	0.43	1.21
NGC4639	31.32±0.3 ¹	55.0	2.510	10.39	10.29	1.66	31.80±0.09	32.25	0.48	0.93
NGC4725	31.15±0.3 ⁷	44.9	2.724	8.31	8.25	1.73	30.57±0.08	30.84	-0.58	-0.31
NGC7331	30.71±0.3 ⁷	69.0	2.712	8.23	7.92	1.72	30.89±0.10	31.39	0.18	0.68

Table 8. The Tully-Fisher parameters for HST Cepheid galaxies with inclinations, $i > 35$ deg. These galaxies' I band TF parameters have been obtained from the work of (1) Pierce (1994), (2) Pierce (priv. comm.) reported by Ciardullo et al (1989), (3) Bureau, Mould & Staveley-Smith (1996) (4) the TF distance for NGC3621 is based on an I_T derived from de Vaucouleurs & Longo (1988) using $(V - I)_{Johnson} = 1.3(V - I)_{KC}$ to convert $I_{Johnson}$ into I_{KC} and an aperture correction of 0.35 mag, giving $I_T=8.83$ mag. (5) The I_T magnitude is from Mathewson & Ford (1996) (6) The I_T magnitude is derived from Sakai et al.(1999) (7) Where the TF distances were unavailable, they have been derived using line-widths, inclinations and V mags from The Third Reference Catalogue (de Vaucouleurs et al., 1991) and V-I mags from Buta & Williams (1995), using the precepts of Tully & Fouque (1985) and Pierce & Tully (1992).

Name	TF Distance	$B - I_{corr}$	$\log W^R_I$	I_{corr}	KP	KP-TF	Corrected	Corr-TF	12+logO/H
M31	24.56±0.3	1.69	2.712	1.77	24.44±0.10	-0.12	24.76	0.20	8.98±0.15
M33	24.23±0.3	1.15	2.322	4.84	24.63±0.09	0.40	24.84	0.61	8.82±0.15
NGC2403	27.40±0.3	1.16	2.411	7.24	27.51±0.15	0.11	27.71	0.31	8.80±0.10
M81	28.10±0.3	1.82	2.685	5.54	27.80±0.08	-0.30	27.97	-0.13	8.75±0.15
NGC3109	25.73±0.3	0.88	2.032	8.87	25.26±0.22	-0.47	24.97	-0.76	8.06±0.15
NGC300	26.35±0.3	0.94	2.284	7.30	26.66±0.10	0.31	26.56	0.21	8.35±0.15

Table 9. The TF parameters for the local calibrators are taken from Pierce & Tully (1992). The KP distances come from Table 3 of Ferrarese et al (2000).

ble to those for the lower linewidth points. If the corrected data are more accurate, then it would suggest that the linewidth correlation in Fig. 14(a) was more likely due to the higher linewidth galaxies having higher metallicity rather than the alternative Malmquist bias explanation previously considered. In this view, the TF distances have a constant offset with the HST Cepheid distances uncorrelated with linewidth.

We now argue that the continuing offset between the HST Cepheid galaxies and the Local Calibrators in Fig. 14(b) may be evidence that the TF distances also require a metallicity correction. The average Cepheid metallicity of the 19 HST galaxies with TF distances is 8.89 ± 0.28 whereas the average Cepheid metallicity of the 6 Local Calibrators is 8.63 ± 0.14 ; only one (M31) has a higher Cepheid metallicity (8.98 ± 0.15) than the HST average. And almost half (7/19) of the HST galaxies have a Cepheid metallicity which is higher than that of Cepheids in the highest metallicity local calibrator, M31. Thus generally, the HST Cepheid galaxies extend to much higher metallicities than the Local Calibrators. In addition, as shown in Fig. 15, there is a strong

4.7σ correlation between TF linewidth and metallicity in the HST/local calibrator TF sample. Even when the lowest linewidth point (NGC3109) is removed the correlation is still a 3.4σ effect. In the HST and Local samples taken individually there is a correlation at the 3σ significance level in both cases. This strong metallicity-linewidth correlation in the 25 galaxy Cepheid-TF sample means that the linewidth-TF residual correlation seen before could actually be caused by a metallicity dependence in the TF relation. The correlations of TF-Cepheid residuals are less strong with metallicity than with linewidth but it is clear that metallicity could plausibly be acting as a third parameter for the TF relation. For example, when Local Calibrators have the same linewidth and metallicity as an HST galaxy then they tend to act consistently and lie in the same part of Fig. 14(b). e.g. M31 and NGC4725 are similar and both lie to the bottom right and the 3 local calibrators and the 4 HST galaxies on the left also have similar metallicities.

Of course, it might not be unexpected that TF distances show a correlation with metallicity. It could be argued that a spiral galaxy with a metallicity which is a tenth of solar will

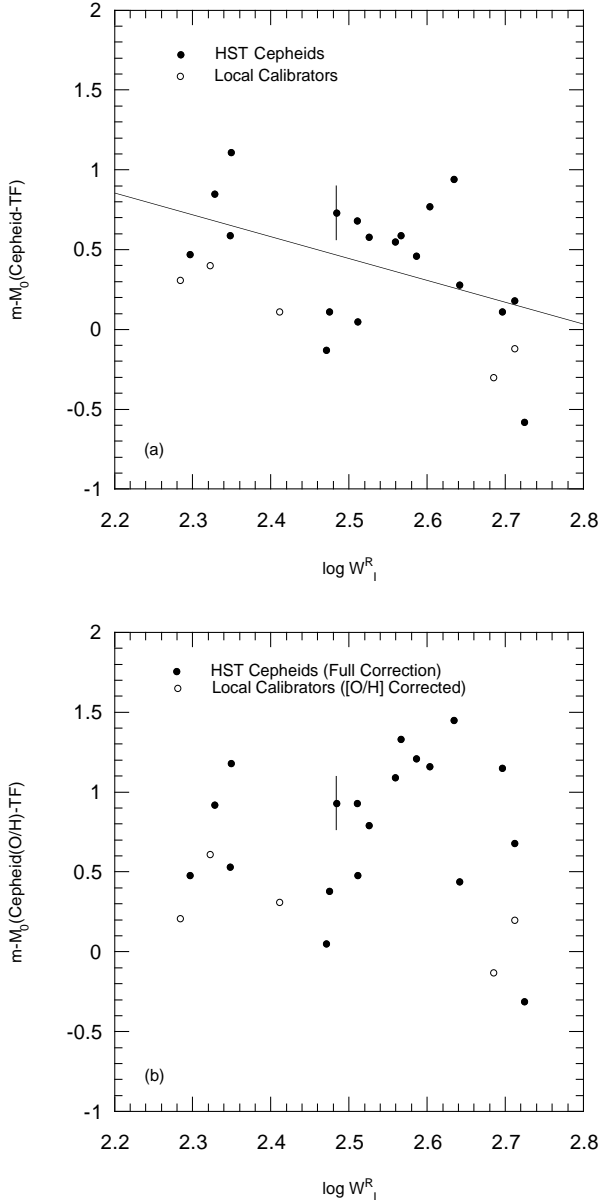


Figure 14. (a) Cepheid-TF residuals plotted against linewidth. A significant correlation is seen in the sense that low linewidth galaxies have bigger residuals. The least-squares line, Cepheid-TF distance modulus difference = $-1.38(\pm 0.68)\log W + 3.88$, is also shown. (b) The same as (a) but now the metallicity corrected Cepheid distances are being used. The correlation is much reduced.

be populated by a main sequence of sub-dwarfs which lies some 0.7mag fainter than a solar metallicity main sequence. On the crude assumption that the same number of stars are formed per unit mass, low metallicity spirals would then form a TF relation which lay parallel but $\approx 0.7\text{mag}$ fainter than for solar metallicity spirals. This may be the underlying explanation of the effects seen in Fig. 14(a,b).

Even though it may have a scale error, the TF route may supply a better estimate of the distance to the Virgo and Fornax cluster mean spiral distances (and hence H_0) because it is thought that the Virgo/Fornax spirals are extended in the line of sight and therefore the average dis-

tance of only a few Cepheid galaxies in these cases may not be very accurate. The Pierce & Tully (1988) TF distance to Virgo is $15.6\pm 1.5\text{Mpc}$ and the Bureau et al. (1996) TF distance to Fornax is $15.4\pm 2.3\text{Mpc}$. Given that TF underestimates corrected Cepheid distances by $46\pm 6.7\%$ at the distance of Virgo/Fornax, this means that the corrected TF distance to Virgo should be $22.8\pm 2.2\text{Mpc}$, similar to the average of the four Virgo core member HST Cepheid distances found above. The corrected TF distance to Fornax is $22.5\pm 3.4\text{Mpc}$, in statistical agreement with the average of three Fornax HST Cepheid distances found earlier. After Shanks (1999), we also include the Ursa Major cluster which has a TF distance of $15.5\pm 1.2\text{Mpc}$ (Pierce & Tully 1988) which is similar to the TF distances for Virgo and Fornax and so within the HST Cepheid range although as yet without actual HST Cepheid observations. The corrected TF distance to Ursa Major is then $22.6\pm 1.8\text{Mpc}$. The heliocentric velocities of these clusters are $1016\pm 42\text{kms}^{-1}$ for Virgo (Pierce & Tully 1988), $1450\pm 34\text{kms}^{-1}$ for Fornax (Bureau et al. 1996) and $967\pm 20\text{kms}^{-1}$ for Ursa Major (Pierce & Tully 1988). Ignoring infall and simply taking the ratio of heliocentric velocity to corrected distance results in values of $H_0 = 45, 64, 43\text{ kms}^{-1}\text{Mpc}^{-1}$ from Virgo, Fornax and Ursa Major respectively. The mean of these results gives $H_0 = 51\pm 7\text{kms}^{-1}\text{Mpc}^{-1}$. Alternatively, assuming an infall model, Pierce & Tully (1988) derived a value of $H_0 = 85\pm 10\text{kms}^{-1}\text{Mpc}^{-1}$ from the Virgo and Ursa Major TF distances. Therefore, under the same assumptions, our corrected TF distances would give $H_0 = 58\pm 7\text{kms}^{-1}\text{Mpc}^{-1}$. However, caution is again required because the continuing large uncertainties surrounding the infall model translate directly into uncertainty in H_0 . All we take from this discussion is that values of H_0 around $50\text{km s}^{-1}\text{Mpc}^{-1}$ or even lower cannot yet be ruled out by considerations of the Cepheid or TF distance scales.

6.3 A Metallicity Dependence for Type Ia Supernovae?

Finally, we show in Fig 16 the effect that a Cepheid metallicity term of the size described here would have on the SNIa ‘standard candle’. There are 8 galaxies with both SNIa and Cepheid distances. Fig. 16(a) shows the plot of SNIa absolute B magnitude vs host galaxy metallicity assuming the apparent magnitudes, Cepheid distance moduli and reddenings of Gibson et al (1999) as summarised in Table 10. Little correlation with metallicity is seen. Fig. 16(b) shows the same graph now with the same data except that the Cepheid distance moduli are corrected for the metallicity effect of Hoyle, Shanks & Tanvir (2001). A correlation with metallicity is now seen. A least squares fit gives the slope as -0.92 ± 0.33 in the sense that higher metallicity galaxies have brighter SNIa.

In fact, we note that there is a correlation between Δm_{15} and metallicity amongst these eight galaxies, in the sense that higher metallicity galaxies have higher Δm_{15} . A least squares fit to this relation gives a slope of 0.284 ± 0.086 . Since the peak-luminosity decline-rate correlation implies that higher Δm_{15} means fainter SNIa luminosities it is clear that if this correlation is real the use of the peak-luminosity decline-rate correlation invokes a bigger metallicity effect in the SNIa luminosities than if it is ignored. When the

Name	M_B (Gibson)	Δm_{15}	$\Delta M(\Delta m_{15})$	$M_B(\Delta m_{15})$	Corr-KP	$M_B(\Delta m_{15})$ -(Corr-KP)
NGC4639	-19.51	1.07	0.02	-19.49	0.45	-19.94
NGC4536	-19.49	1.10	0.00	-19.49	0.36	-19.85
NGC3627	-19.25	1.31	-0.20	-19.45	0.50	-19.95
NGC3368	-19.51	1.01	0.06	-19.45	0.28	-19.73
NGC5253	-19.40	0.87	0.11	-19.29	-0.23	-19.06
IC4182	-19.74	0.87	0.11	-19.63	-0.06	-19.57
NGC4496	-19.20	1.06	0.03	-19.17	0.18	-19.35
NGC4414	-19.66	1.11	-0.01	-19.67	1.04	-20.71

Table 10. The SNIa peak absolute B magnitude M_B and the Δm_{15} parameters are taken from Gibson et al. (2000). $\Delta M(\Delta m_{15})$ is the correction for Δm_{15} from equation (1) of Gibson et al.(2000), ignoring the reddening correction to Δm_{15} which is small.

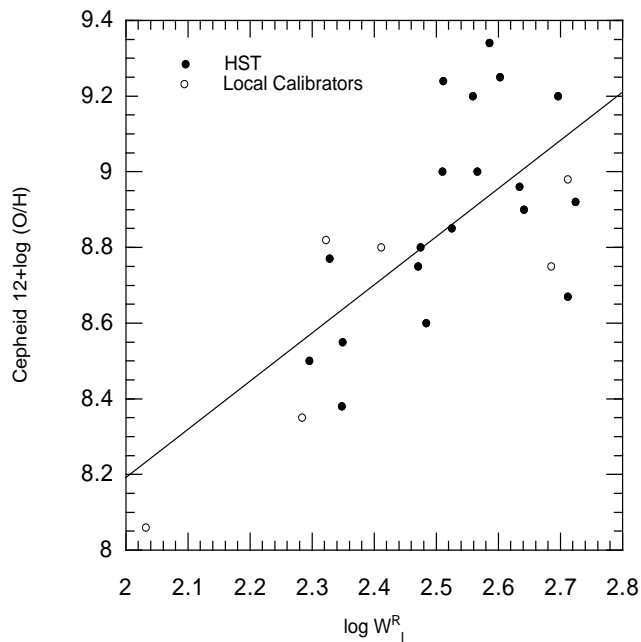


Figure 15. The metallicity-linewidth correlation for the HST Cepheid galaxies. The least-squares fitted line, $12 + \log(O/H) = 1.274(\pm 0.268)\log W_I + 5.643$, is also shown.

metallicity correction of Hoyle, Shanks & Tanvir (2001) is applied without the Δm_{15} correction, the slope of the peak luminosity-metallicity correlation reduces from -0.92 ± 0.33 to -0.75 ± 0.34 .

Now it might be argued that the fact that the Δm_{15} correction works only to accentuate the effect of metallicity on Type Ia luminosity means that the empirically determined decline rate correlation is evidence against a strong metallicity effect for SNIa. However, the decline rate correction is much smaller than the proposed metallicity correction which would be dominant. Also, the selection effects induced by the wide dispersion in SNIa luminosity would have to be carefully taken into account before coming to any conclusion. For example, SNIa surveys at intermediate redshifts would preferentially detect the brighter SNIa in higher metallicity galaxies, leading to SNIa which were systematically too bright relative to local SNIa and with an artificially too small dispersion. There would also be a potentially serious impact on the SNIa Hubble Diagram determinations of q_0 ; if the average metallicity of galaxies was a factor of 3 lower at

$z > 0.5$ than observed locally then the SNIa would on average be ≈ 0.3 mag fainter than expected and this is order of the amount needed to explain away the positive detection of the cosmological constant by the Supernova Cosmology teams (Perlmutter et al 1999, Schmidt et al 1998).

7 CONCLUSIONS

After a detailed analysis of the relationship between the dispersion in Cepheid P-L relations and metallicity, it can be inferred that there is a relationship in the V-band at the level 0.10 ± 0.03 mag dex $^{-1}$, in the sense that the dispersion about the P-L relation increases with metallicity. This is a good fit and significant at the 3σ level and may arise because high metallicity galaxies contain Cepheids with a wider range of metallicities and hence luminosities. The reason that a less strong relationship is observed in the I-band is unclear. It could be that metallicity effects are less significant in the I-band or that a relationship with the same slope but a lower amplitude is masked in I because of the effect of photometry/crowding errors on the intrinsically tighter dispersion. The size of the dispersion metallicity correlation that we find is roughly consistent with the global P-L metallicity dependence of $\Delta M/[O/H] = -0.66$ mag dex $^{-1}$ claimed by Hoyle, Shanks & Tanvir (2001).

The first consequence of this is that there is now more evidence that a global metallicity correction should be applied to Cepheid distances. The second consequence is that the effects of incompleteness bias may also be important, especially for high metallicity galaxies at large distances. These results combined imply that Cepheid distance moduli are too short on the average by 0.29 ± 0.21 mag and by up to ≈ 0.5 mag in the case of the distant high metallicity galaxies.

We have described the effects on the distance scale if the metallicity corrections to Cepheid distances suggested here prove accurate. We have shown that the distances to the Virgo galaxy cluster increase from 16.6 to 20.9 Mpc. We have shown that there would be a significant scale error in the TF scale which would mean that the TF relation underestimates distances by 46% at the distance of Virgo. We have suggested that this may be due to the high metallicity of the HST Cepheid galaxies compared to the Local Calibrators and that metallicity may act as a significant second parameter in the TF relation.

We have shown by correcting TF distances to the Virgo, Fornax and Ursa Major clusters that this leads to a range of

/cos/h/pallen/plplots/

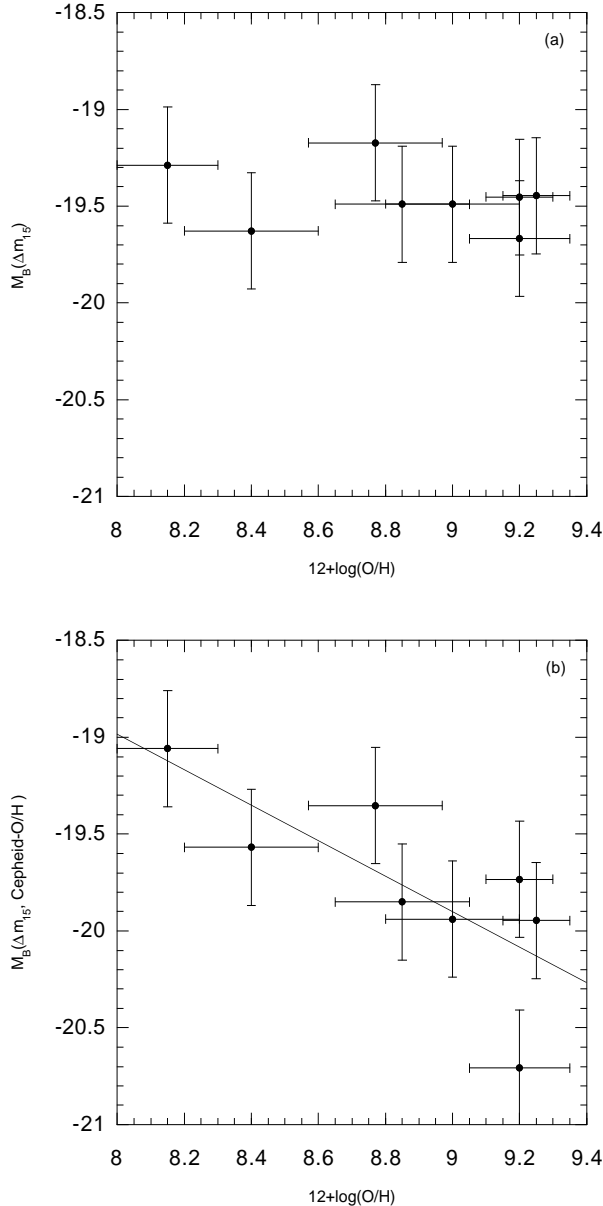


Figure 16. (a) The SNIa absolute magnitude-metallicity relation using the SNIa peak magnitudes of Gibson et al, corrected for Δm_{15} as in Table 10. (b) The SNIa absolute magnitude-metallicity relation using the SNIa peak magnitudes of Gibson et al. (2000), now corrected for Δm_{15} and metallicity as in Table 10. The least-squares fitted line, $M_B = -0.92(\pm 0.33)\log W - 11.65$, is also shown.

values of H_0 between $43\text{--}64 \text{ km s}^{-1}\text{Mpc}^{-1}$ if no infall model is assumed and a value of $H_0=58\pm 7 \text{ km s}^{-1}\text{Mpc}^{-1}$ if an infall model is assumed, although the infall model itself is highly uncertain. We have also shown that if the Cepheid luminosities are metallicity dependent then so are the peak luminosities of Type Ia supernovae. New information on the metallicity of Type Ia supernovae at both intermediate and high redshifts will be needed before conclusions on supernova estimates of H_0 and q_0 can be drawn.

Of course, Cepheids with or without metallicity corrections provide no direct check on the secondary distance in-

dicators that are purely associated with early-type galaxies such as SBF, PNLF or fundamental plane indicators. Therefore we simply note that the early-type route to H_0 through the Leo-I Group (Tanvir et al 1995, Tanvir et al 1999), which is the most nearby galaxy group containing both spirals with HST Cepheids and early-type galaxies is that our corrected distance to Leo-I of $12.5\pm 0.3 \text{ Mpc}$ from the $11.2\pm 1.0 \text{ Mpc}$ quoted by Tanvir et al (1999) is that the derived value of H_0 will therefore decrease from $H_0=67\pm 7 \text{ km s}^{-1}\text{Mpc}^{-1}$ to $H_0=60\pm 6 \text{ km s}^{-1}\text{Mpc}^{-1}$. But this estimate depends on using secondary distance indicators to obtain the Coma-Leo relative distance and it would be surprising if the metallicity corrections etc. were only found to be important for the spiral distance indicators!

We therefore believe that there is increasing evidence that Cepheid distances require significant corrections for the effects of metallicity and incompleteness bias with important potential consequences for the distance scale, Hubble's Constant and cosmology. Further tests of the metallicity dependence of the Cepheid P-L relation include a study of the metallicity of the main-sequence stars in the open cluster NGC7790 (Hoyle & Shanks 2001). We are also using our metallicity-corrected Cepheid distances to make new checks of dynamical infall models into Virgo and Fornax (Shanks and Warfield in prep.). Ultimately, a full understanding of the metallicity effects on Cepheids and so the value of Hubble's Constant may require parallaxes to Galactic Cepheids outside the Solar Neighbourhood from astrometry satellites such as GAIA and a larger sample of Cepheids in galaxies with a wide range of metallicities from instruments such as the HST Advanced Camera and the NGST fitted with a Visible Camera.

ACKNOWLEDGMENTS

We thank the HST Distance Scale Key Project for making their Cepheid data publicly available. PDA thanks the University of Durham for support.

REFERENCES

- Bureau, M., Mould J.R. & Staveley-Smith, L. 1996, ApJ, 463, 60
- Buta, R. & Williams, K.L., 1995, AJ, 105, 543
- Cardelli, J. A. et al, 1989, ApJ, 345, 245
- Ciardullo, R., Jacoby, G.H., & Ford, H.C., 1989, ApJ, 344, 715
- de Vaucouleurs, G. et al 1991 Third Reference Catalogue of Bright Galaxies, Springer-Verlag
- de Vaucouleurs, A., & Longo, G. 1988 Catalogue of Visual and Infrared Photometry of Galaxies From 0.5 Micron to 10 micron (1961-1985).
- Feast, M. W. and Catchpole, R. M., 1997, MNRAS, 286, L1
- Ferrarese, L. et al, 1996, ApJ, 464, 568
- Ferrarese, L. et al, 1998, ApJ, 507, 655
- Ferrarese, L. et al, 2000, ApJS, 128, 431
- Ferrarese, L. et al, 2000, PASP, 112, 177
- Freedman, W. L., 1994, ApJ, 427, 628
- Gibson, B. K. et al, 1999, ApJS, 128, 431.
- Gibson, B. K. et al, 1999b, ApJ, 512, 48
- Gibson, B. K. et al, 2000, ApJ, 529, 723
- Graham, J. A. et al, 1997, ApJ, 477, 535
- Gould, A.J. & Popowski, P. 1997 astro-ph/9702202
- Graham, J. A. et al, 1999, ApJ, 516, 626

- Hoyle, F., Shanks, T. & Tanvir, N.R., 2001, MNRAS *submitted*
(astro-ph 0002521)
- Hoyle, F. & Shanks, T., 2001, *in prep.*
- Hughes, S. M. G. et al, 1998, ApJ, 501, 32
- Kelson, D. D. et al, 1996, ApJ, 463, 26
- Kelson, D. D. et al, 1999, ApJ, 514, 614
- Kennicutt, R. C. et al, 1998, ApJ, 498, 181
- Kochanek, C., 1997, ApJ, 491, 93
- Macri, L. M. et al, 1999, ApJ, 521, 155
- Macri, L. M., Huchra, J.P., Sakai, S., Mould, J.R. & Hughes, S.M.G., 2000, ApJS, 128, 461
- Madore, B. F. and Freedman, W. L., 1991, PASP, 103, 667
- Mathewson, D.S. and Ford, V. L., 1996, ApJS, 107, 97
- Mochejska, B. J., Macri, L. M., Sasselov, D. D. & Stanek, K. Z., 2000, ApJ, 120,810
- Mould, J. R. et al, 2000, ApJ, 528, 655
- Musella, I., Piotto, G. & Cappaccioli, M. 1998, AJ, 114, 976
- Oey, M. S. and Kennicutt, R. C., 1993, ApJ, 411,137
- Pierce, M. J. and Tully, B., 1988, ApJ, 330, 579
- Pierce, M.J. and Tully, R.B., 1992 ApJ, 387, 47
- Pierce, M. J., 1994, ApJ, 430, 53
- Perlmutter, S. et al, 1999, ApJ, 517, 565
- Phelps, R. et al, 1998, ApJ, 500, 763
- Press, W. H. et al, Numerical Recipes in Fortran: The Art of Scientific Computing 2nd Edition, 1992, CUP
- Prosser, C. F. et al, 2000, ApJ, 525, 80
- Rawson, D. M. et al, 1997, ApJ, 490, 517
- Ratcliffe, A. et al, 1996, MNRAS, 281, 47
- Saha, A. Labhardt, L. & Prosser, C., 2000, PASP, 112, 163
- Sakai, S. et al, 1999, ApJ, 523, 540
- Sandage, A. R., 1958, ApJ, 127, 513
- Sandage, A. R., PASP, 1988, 100 ,935
- Sandage, A. R., ApJ, 1994, 430, 13
- Sandage, A. R., ApJ, 1996, 460, L15
- Sasselov, D. D. et al., 1997, A&A, 324, 471
- Schlegel, D. J. et al., 1998, ApJ, 500, 525
- Schmidt, B. P. et al, 1998, ApJ, 507, 46
- Shanks, T., 1997, MNRAS, 290, L77
- Shanks, T., 1999, In Harmonising Cosmic Distance Scales, eds Egret D. & Heck, A., PASP, pp. 230-234
- Silbermann, N. A. et al, 1996, ApJ, 470, 1
- Silbermann, N. A. et al, 1999, ApJ, 515, 1
- Tanvir, N. R., Ferguson, H.C. & Shanks, T. , 1999, MNRAS, 310, 175
- Tanvir, N. R., Shanks, T., Ferguson, H.C. & Robinson, D.R.T. 1995, Nature, 377, 27
- Tanvir, N. R., 1998, In Harmonising Cosmic Distance Scales, eds Egret D. & Heck, A., PASP, pp. 84-100
- Tully, R.B. & Fouque, 1985, ApJS, 58, 67
- Turner, A. et al, ApJ, 505, 207
- Webb, S., Measuring the Universe: The Cosmological Distance Ladder, 1997, Springer-Praxis